Global and Planetary Change 206 (2021) 103624

Contents lists available at ScienceDirect

Global and Planetary Change

journal homepage: www.elsevier.com/locate/gloplacha

Five-fold expansion of the Caspian Sea in the late Pliocene: New and revised magnetostratigraphic and $^{40}Ar/^{39}Ar$ age constraints on the Akchagylian Stage

S. Lazarev [a,1,*], K.F. Kuiper [b], O. Oms [c], M. Bukhsianidze [d], D. Vasilyan [e,f], E.L. Jorissen [a], M. J. Bouwmeester [a], V. Aghayeva [g,h], A.J. van Amerongen [a], J. Agustí [i,j,k], D. Lordkipanidze [d], W. Krijgsman [a]

[a] Paleomagnetic Laboratory «Fort Hoofddijk», Department of Earth Sciences, Utrecht University, Budapestlaan 17, 3584 CD Utrecht, the Netherlands
[b] Department of Earth Sciences, Faculty of Science, Vrije Universiteit Amsterdam, De Boelelaan 1085, 1081HV Amsterdam, the Netherlands
[c] Facultat de Ciències Universitat Autònoma de Barcelona, 08193 Bellaterra, Barcelona, Spain
[d] Georgian National Museum, Purtseladze Street 3, Tbilisi 0105, Georgia
[e] Department of Geosciences, University of Fribourg, Chemin de Musée 4, 1700 Fribourg, Switzerland
[f] JURASSICA Museum, Porrentruy, Route de Fontenais 21, 2900 Porrentruy, Switzerland
[g] Department of Applied Geosciences and Geophysics, University of Leoben, Peter-Tunner-Straße 5, 87000 Leoben, Austria
[h] Institute of Geography, Azerbaijan National Academy of Science, Huseyn Javid Avenue 151, AZ1143 Baku, Azerbaijan
[i] Institut Català de Paleoecologia Humana i Evolució Social (IPHES), Zona Educacional 4, Campus Sescelades URV (Edifici W3), 43007 Tarragona, Spain
[j] Universitat Rovira i Virgili, Departament d'Història i Història de l'Art, Avinguda de Catalunya 35, 43002 Tarragona, Spain
[k] Institució Catalana de Recerca i Estudis Avançats (ICREA), Pg. Lluís Companys 23, 08010 Barcelona, Spain

ARTICLE INFO

Editor: Haywood Alan

Keywords:
Caspian Basin
Plio–Pleistocene
Akchagylian
Magnetostratigraphy
$^{40}Ar/^{39}Ar$ chronology
Kvabebi
Kushkuna

ABSTRACT

The Global climate reorganisation in the late Pliocene linked to enhancement of the Atlantic Ocean Thermohaline Circulation (AOTC), instigated a transition to glacial-interglacial cyclicity in the Quaternary. Enhancement of the AOTC amplified atmospheric precipitation over the Eurasian interior strengthening Northern Hemisphere Glaciation. Increased rainfall on the vast Russian Plain drained into the endorheic Caspian Sea, which makes the Caspian geological record highly potential for tracing atmospheric precipitation changes. Two major palaeohydrological events in the Caspian Sea, the Akchagylian transgression and the Akchagylian marine incursion, led to a five-fold enlargement of the Caspian Sea surface area and transformed the basin palaeoecology, enabling active interregional faunal dispersals. The Akchagylian Stage still lacks an unequivocal age model with two age constraints – the "long Akchagylian" (3.6–1.8 Ma) and the "short Akchagylian" (2.7–2.1 Ma) standing on magnetostratigraphic studies of geological records in Turkmenistan and the Kura Basin, respectively. The age discrepancies also exist within the Kura Basin, where the fossil mammal-bearing Kvabebi locality with Akchagylian marine fauna was magnetostratigraphically dated at 3.2 Ma. In this paper, we try to resolve the age contradictions for the Akchagylian Stage. We revisit the Kvabebi (Georgia) and Kushkuna (Azerbaijan) sections of the western Kura Basin and provide new magnetostratigraphic and $^{40}Ar/^{39}Ar$ age constraints on these marginal Akchagylian deposits. Moreover, we revise the magnetostratigraphy of 25 geological records from Turkmenistan and the Kura Basin and propose a new unified age model for the Akchagylian Stage: 1. Intrabasinal Akchagylian freshwater-mesohaline transgression at 2.95 ± 0.02 Ma; 2. Akchagylian marine incursion through establishment of a Caspian-Arctic connection (2.75–2.45 Ma); 3. Akchagylian–Apsheronian boundary highlighting a Caspian-Black Sea connection at 2.13 Ma. The sudden expansion of the Caspian Sea at 2.95 ± 0.02 Ma potentially correlates to the interglacial intensification of the AOTC between 2.95 and 2.82 Ma. The new ages constrain a much shorter (2.95–2.1 Ma) Akchagylian than in previously mentioned regional geological time scales (3.6–1.8 Ma) and strongly appeal to reconsider the ages of numerous archaeological and mammalian sites in the Caspian region.

* Corresponding author.
E-mail address: sergei.lazarev@unifr.ch (S. Lazarev).
[1] Currently at the Department of Geosciences, University of Fribourg, Chemin de Musée 6, 1700 Fribourg, Switzerland.

https://doi.org/10.1016/j.gloplacha.2021.103624
Received 25 March 2021; Received in revised form 10 August 2021; Accepted 24 August 2021
Available online 28 August 2021

1. Introduction

In the late Pliocene, the global climatic system underwent remarkable reorganisations that triggered the glacial-interglacial cycles of the Quaternary. Gradual closure of the Panama Isthmus and enhancement of the Atlantic Ocean Thermohaline Circulation (AOTC) played a key role in the initiation of Northern Hemisphere Glaciation (NHG) (Haug and Tiedemann, 1998; Bartoli et al., 2005). Reorganisation of the AOTC increased atmospheric precipitation in the Eurasian interior (i.e. in Western Siberia) that consequently led to freshening of the Arctic Ocean and Northern Hemisphere cooling (Driscoll and Haug, 1998).

Late Pliocene atmospheric precipitation changes in northern Eurasia are difficult to unravel from local records due to the lack of suitable geological successions. Rainfall on the Russian Plain was mostly transported to the catchment area of the endorheic Caspian Sea whose water budget is highly sensitive to changes of freshwater input. This makes the Caspian geological record highly suitable to trace and date the climatic changes in northern Eurasia. However, the palaeoenvironmental reconstructions of the Caspian Sea still lack unequivocal age constraints, hindering the understanding of the hydrological dynamics of the Pliocene-Pleistocene climate transition.

During the Pliocene to Quaternary, major sea-level variations of

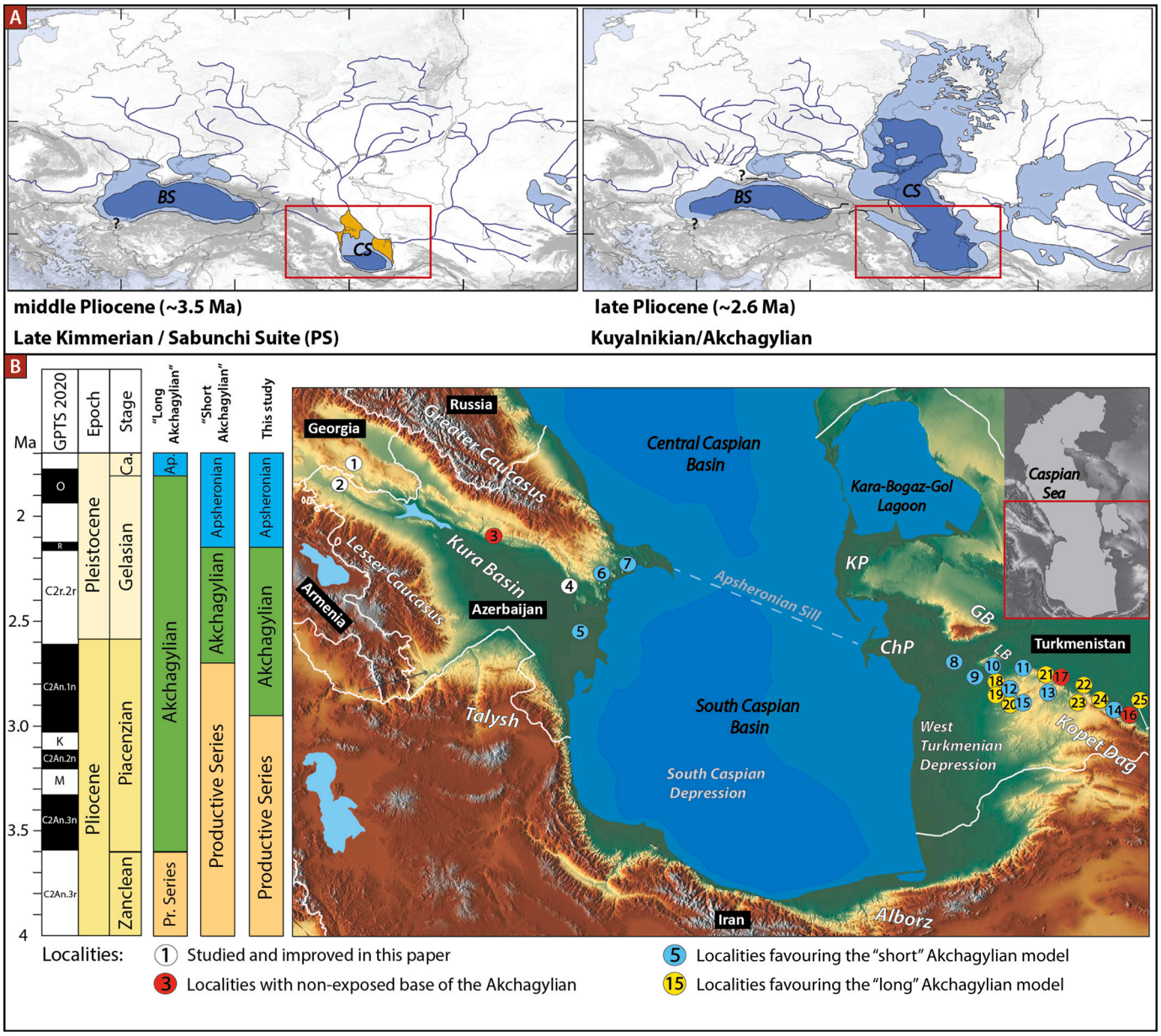

Fig. 1. Palaeogeographic reconstructions, geological time scale and topographic locality map of studied and revised sections in the Caspian Basin. A. middle Pliocene and latest Pliocene–Early Pleistocene west Eurasian continental interior. After Krijgsman et al. (2019) and van Baak et al. (2019) based on maps by Vinogradov (1969) and Abdullayev et al. (2012); B. Studied (1 – Kvabebi, 2 – Kushkuna, 4 – Hajigabul) and revised localities across the Kura Basin (3 – Goychay, 5 – Babazanan, 6 – Jeirankechmez, 7 – Lokbatan) and the Turkmenian coast (8 – Monzhukly, 9 – Boyadag, 10 – Portsayman, 11 – Bayram, 12 – Yagut, 13 – Adzhidere, 14 – Beurme, 15 – Kotura, 16 – Archman, 17 – Ushak, 18 – Gokchadere, 19 – Issu, 20 – Kushuldzha, 21 – Orumeldzha, 22 – Diodzhi, 23 – Pyrnuar, 24 – Zau, 25 - Khalats). Columns on the left: Geomagnetic polarity time scale (GPTS 2020), Epoch/Age (Raffi et al., 2020) and regional stages. Regional Stages: a* classical definition (Shantser, 1982; Arslanov et al., 1988; Nevesskaya et al., 2003; Gladenkov, 2018), b* (Lazarev et al., 2019; van Baak et al., 2019). Abbreviations used on the figures: A. BS – Black Sea; CS – Caspian Sea; PS – Productive Series; B. KP – Krasnovodsk Peninsula; ChP – Cheleken Peninsula; LB – Lesser Balkhan; GB – Greater Balkhan. The map base is taken from www.maps-for-free.com.

several hundreds of meters have been inferred for the endorheic Caspian Basin (Popov et al., 2006; Svitoch, 2014; Krijgsman et al., 2019). A dramatic Pliocene base-level drop is expressed by the progradation of the palaeo-Volga Delta into the South Caspian Basin (Fig. 1a), forming the massive hydrocarbon reservoirs of the Pliocene Productive Series in Azerbaijan (Reynolds et al., 1998; Kroonenberg et al., 2005; Abdullayev et al., 2012). These deltaic sandstones are subsequently sealed by mostly fine-grained deposits of the Akchagylian stage.

The Akchagylian transgression triggered one of the most extreme sea-level rise events in the Caspian Basin. It increased the Caspian Sea surface area five-fold, covering vast areas of present-day southern Russia, Central Asia and the Caucasian Kura foreland basin in Azerbaijan (Fig. 1a). Recent palaeontological and geochemical investigations showed that Akchagylian water-level rise was followed by the invasion of marine waters, likely via a connection to the Arctic Ocean, known as the Akchagylian flooding (Richards et al., 2018; Bista, 2019; van Baak et al., 2019). The usage of both terms "transgression" and "flooding" however, remains highly confusing due to the their similar meaning. In this study, we distinguish these two events as the *Akchagylian transgression* and the *Akchagylian marine incursion* respectively that better describes their nature.

Palynological analyses indicate that lake expansion influenced regional climate and vegetation, especially by making Quaternary glacial episodes milder (Hoyle et al., 2020). The Akchagylian expansion of the Caspian Basin and its connection with the global ocean also contributed to the rise of unique faunal communities with new ostracod, foraminifera, dinoflagellate cyst (dinocyst) and mollusc taxa (e.g. Krijgsman et al., 2019 and references therein).

Despite a relatively good understanding of the Akchagylian transgression's impact, there is no unequivocal age constraint for the Akchagylian Regional Stage. Two major age models exist for the Akchagylian: the "short Akchagylian" (~2.7–2.1 Ma) and the "long Akchagylian" (3.6–1.8 Ma).

The short Akchagylian model is based on the correlation of the lower Akchagylian boundary to the upper Gauss (C2An.1n) chron (Khramov, 1960, 1963; Lazarev et al., 2019; van Baak et al., 2019). The $^{40}Ar/^{39}Ar$ dating of volcanic ashes in the Kura Basin with ages between 2.73 and 2.65 Ma confirmed this correlation and expressed the high volcanic activity in this time interval (Hoyle, 2019; van Baak et al., 2019) Consequently, $^{40}Ar/^{39}Ar$ geochronology, along with high-resolution dinocyst studies dates the Akchagylian marine incursion at 2.75 Ma (Hoyle et al., 2021). Yet, no age determination has been provided for the initial Akchagylian transgression. The top of the Akchagylian (the Akchagylian-Apsheronian boundary) was defined in the Hajigabul section by the first occurrence of indicative Apsheronian molluscs like *Monodacna* sp., and *Apscheronia* sp. (Lazarev et al., 2019). There, this interval was magnetostratigraphically correlated to the Reunion (C2r.1n) subchron, and thus dated at 2.13 Ma (Lazarev et al., 2019). This resulted in a total duration of 620 kyr for the Akchagylian stage.

The Kvabebi section, located at the western margin of the Kura Basin in Georgia, is an outlier to the short Akchagylian model. This section is renowned for its rich large mammalian fossil fauna intercalated with strata comprising Akchagylian molluscs (Vekua, 1972; Agustí et al., 2009; Bukhsianidze and Koiava, 2018). The Kvabebi mammal site was previously magnetostratigraphically dated in a short reversed polarity interval attributed to C2An.1r (Kaena), providing the age of 3.07 Ma (Agustí et al., 2009). Stratigraphically below, the Akchagylian mollusc fauna is found in a normal polarity interval, correlated to C2An.2n and dating back to ~3.2 Ma (Agustí et al., 2009). Volcanic ash layers at the basal part of the Kvabebi section can be used to evaluate the age controversy. However, no radio-isotopic age datings have been published so far from these tephras.

All this is in significant contrast to the "long Akchaylian" model used in the standard regional geological time scale (Nevesskaya et al., 2003; Nevesskaya et al., 2004; Gladenkov, 2018). This model is derived from magnetostratigraphic correlations of several sections in the Kopet-Dag area of western Turkmenistan (Trubikhin, 1977). In some sections, the base of Akchagylian was found within a long normal chron with two tiny reversed subchrons interpreted as Kaena (C2An.1r) and Mammoth (C2An.2r) subchrons. The onset of the Akchagylian was correlated to the base of the Gauss chron, nowadays dated at 3.6 Ma (Raffi et al., 2020). The top of Akchagylian has been placed at the top of the Olduvai subchron at the age of 1.8 Ma. This results in a total duration of 1.8 Myr for the Akchagylian, approximately three times longer than the "short Akchagylian" model suggests.

The strong contradiction between the two age models complicates biogeographic, palaeoclimatic and archaeological studies in the region, and a unified age model is highly needed. In this paper, we revisited and resampled the Kvabebi section in Georgia with a higher resolution and re-measured samples from the study of Agustí et al., 2009. For comparison, we also dated the neighbouring Kushkuna section located ~27 km SW from Kvabebi in Azerbaijan. Moreover, we established $^{40}Ar/^{39}Ar$ ages of three volcanic ash samples from the Kvabebi and Hajigabul sections that allowed to confirm and solidify previously proposed magnetostratigraphic correlations. Hence, we resolve the age contradictions within the Kura Basin and revise the previous geochronological constraints for the Akchagylian stage. The new age constraints from the Kura Basin were then compared with those from the Kopet-Dag, which results in a new revised comprehensive age model for the Akchagylian Stage in the entire Caspian region. The new age constraints also allow to look at the palaeogeographic evolution of the Caspian Sea under the scope of the late Pliocene global climate changes and provide new data for further palaeoclimatic reconstructions.

2. Geological background

The Caspian Sea is a N-S elongated endorheic basin at the crossroads of Europe and Asia. The Caspian Sea overlies three tectonic-structural zones that determine the sea's subdivision into three basins: North, Middle and South Caspian. The North and Middle Caspian basins are situated on the tectonically stable Eurasian and Scythian plates (Khain et al., 2004), while the South Caspian Basin belongs to the Alpine-Himalayan orogenic belt and is the most tectonically active part of the Caspian Sea (Jackson et al., 2002).

The late Cenozoic tectonic history of the South Caspian Basin has been driven by the continent-continent collision between the Arabian and Eurasian plates and is expressed by numerous thrust-fold ridges (Allen et al., 2002; Allen et al., 2003). On the S-SW, the South Caspian Basin is delimited by the Talysh and Alborz mountains. The northern margin of the basin is defined by the 850 km long NW–SE striking mountain range of the Greater Caucasus. The latter extends eastward into the Caspian Sea, forming the Apsheron Sill between the Middle and South Caspian basins. Further southeast, the ridge extends into the Kopet-Dag ridge of West Turkmenistan (Fig. 1B).

The central part of the South Caspian Basin hosts the major depocenter – the South Caspian Depression that consists of a rigid ?oceanic-type basement and up to 20-km-thick sedimentary cover (Mangino and Priestley, 1998). To the west, the South Caspian Basin extends into the Kura Basin – a foreland basin between the Lesser and Greater Caucasus. The eastern margin of the South Caspian Basin comprises the West Turkmenian Depression, which forms a gradually-thickening eastward-extension of the South Caspian basement (Mangino and Priestley, 1998; Jackson et al., 2002).

A major tectonic and palaeogeographic reorganisation in the Caspian region happened during the Mio-Pliocene transition. Amplification of Arabian-African-Eurasian collision provoked northward subduction of the South Caspian basement, which led to a rapid increase of subsidence (Allen et al., 2002). The actively subsiding South Caspian and Kura basins accumulated about 8 and 10 km of sediments since the Pliocene, respectively (Allen et al., 2002). At the same time, regional shortening and a climatically-driven water-level drop in the Eastern Paratethys led to the closure of the Ciscaucasian Strait and isolation of the Caspian Sea

from the Black Sea region (Popov et al., 2006). The following disruption of the Caspian basin hydrological budget resulted in a substantial water-level drop shrinking the surface area of the Caspian Sea down to the size of the South Caspian Depression (Fig. 1A) (Krijgsman et al., 2010; Popov et al., 2010; van Baak et al., 2016). This lowstand period was marked by a progradation of the main regional deltas over the largely dessicated Middle and North Caspian Basin into the South Caspian Basin. Here, Palaeo-Amu-Darya, Palaeo-Volga and Palaeo-Kura formed up to 7-km-thick sedimentary record in the basin interior (Morton et al., 2003; Kroonenberg et al., 2005; Torres, 2007). These fluvial-deltaic deposits are known as the "Productive Series" in the Kura Basin (Aliyeva, 2005; Vincent et al., 2010) and as the "Red Colour Formation" in Turkmenistan, also locally recognized as the "Cheleken Suite" or as the "Toronglinks Suite" (Trubikhin, 1977; Vereshchagin, 1982; Torres, 2007). Stratigraphic analogues of this age in the North Caspian region remain unclear and/or are reported as missing.

The lowstand of the Productive Series has been reported to end with the so-callled Akchagylian flooding (Akchagylian marine incursion) characterised by occurrence of new meso- to euhaline faunistic groups (van Baak et al., 2019). This event was explained as the establishment of a hydrological connection between the Caspian Sea and the global ocean, often assumed to run via north with the Arctic ocean (Richards et al., 2018), although no evidence for such connection is found in geological records.

During the Quaternary, the hydrological budget of the Caspian Sea generally stabilised, showing obliquity-driven (41 kyr) water-level

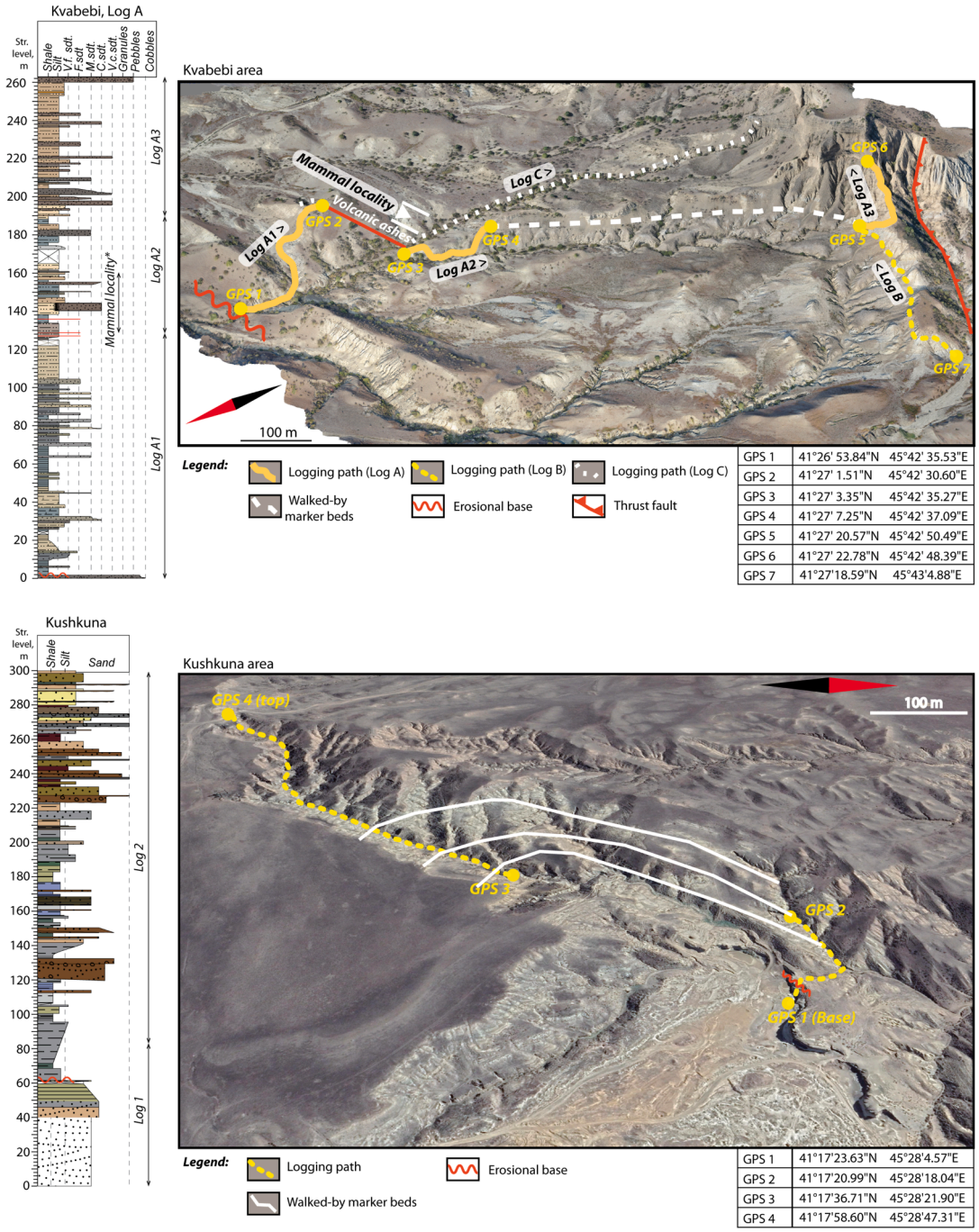

Fig. 2. Composite Log A and 3D model of the Kvabebi locality and composite log and aerial photo (Google Earth) of the Kushkuna locality with the indication of logging paths and GPS coordinates.

oscillations that switched to glacial-interglacial (100 kyr) control at the Early-Middle Pleistocene transition (Jorissen et al., 2019). The astronomically-driven fluctuations were periodically accompanied by large-scale transgressions (e.g. Bakunian, Khvalynian) followed by the establishment of a hydrological connection between the Caspian Sea and the Black Sea through the Manych Strait (Svitoch et al., 2010; Krijgsman et al., 2019). Each of these transgressions was usually followed by an increase of salinity (saline water incursion) and the introduction of new aquatic faunal groups from the Black Sea (Svitoch, 2014; Lazarev et al., 2019).

3. Sections in the western Kura Basin

3.1. Kvabebi section (Georgia)

The Kvabebi section outcrops on a hillside near the Iori River, 17 km southwest from the hamlet of Kvemo Bodbe in the Kakheti region of Eastern Georgia (Figs. 1, 2). Here, the Akchagylian deposits transgressively overlie late Miocene continental conglomerates (Shiraki Suite). The upper parts are bounded by a thrust fold (Ali-Zade et al., 1972). The Kvabebi section is known for its vertebrate fossil faunas attributed to the Ruscinian–early Villafranchian, late Pliocene–Pleistocene (Vekua, 1972; Agustí et al., 2009). The Akchagylian age of the site has been defined by Akchagylian indicative molluscs like *Avimactra subcaspia* and *Cerastoderma* (*Cardium*) *dombra* (Djikia, 1968). The magnetostratigraphic study of Agustí et al. (2009) revealed four magnetochrons: two long normal chrons (N1 and N2) separated by a short reversed chron (R1) and a long reversed chron (R2) in the upper part of the section. N1 and N2 have been correlated to C2An.2n and C2An.1n with R1 and R2 to C2An.1r (Kaena) and C2r.2r (lower Matuyama), respectively.

3.2. Kushkuna section (Azerbaijan)

The Kushkuna section is located 20 km north of the town of Aghstafa in western Azerbaijan, near the sand-quarry next to Ceyrançöl village (Figs. 1, 2). The section is exposed in the NE-flank of an anticline whose hinge is gently plunging to 127°SE. Here, upper Miocene greywacke sandstones are transgressively overlain by Akchagylian mudstones. The previously described 400-m-thick section was built up of two distinct parts. The lower 220 m contains a characteristic Akchagylian mollusc fauna with *Cerastoderma* (*Cardium*) *dombra*, *Avimactra subcaspia* and *Potamides caspium* (Lebedeva, 1972). The upper 180 m comprise continental sandstones and palaeosols that were attributed to an undetermined Akchagylian–Apsheronian age (Ali-Zade et al., 1972; Lebedeva, 1972; Tesakov, 2004). Remains of large and small mammalian faunas from the lower part of the section are attributed to the Villanyian and the MN 16b zone (~3.0–2.5 Ma) (Lebedeva, 1972; Tesakov, 2004). A previous magnetostratigraphic study of the section revealed a single polarity transition from normal to reversed, correlated to the Gauss–Matuyama boundary at the age of 2.6 Ma (Zubakov and Kochegura, 1976).

4. Methodology

4.1. Logging

The stratigraphic thickness has been measured using a Jacob's staff. During logging, basic observations on the colour, lithology, sedimentary structures and faunal content have been documented.

The Akchagylian deposits in the Kvabebi area are well-exposed along numerous gullies. For better coverage of the section and correlation with existing studies, we logged the Kvabebi section along three transects. Moreover, the area has been photographed using a drone, and consequently, a high-resolution 3D model of the site has been built (Fig. 2). The first, 263-m-thick transect named log A covers the entire section in N–NE direction, from the contact of Akchagylian claystones with late Miocene conglomerates at the base (GPS 1) to the top of the section, where Akchagylian conglomerates are delimited by a thrust fold (GPS 6, Fig. 2). The second, 167-m-thick transect called Log B stretches out in SE–NW direction and starts directly with Akchagylian claystones (GPS 7, Supplementary 1). Log C is a 172-m-thick succession previously published by Agustí et al., 2009. Correlation between the logs A, B and C is demonstrated on the correlation scheme (Supplementary 2).

The Kushkuna section has been logged along two separate transects (Fig. 2). The lower part is 110 m thick and encloses Sarmatian (?) sandstones (0–60 m) followed by transgressively overlying Akchagylian mudstones (60–110 m, Fig. 2). The upper part of the section (110–260 m) has been logged in a neighbouring valley after a correlation was established by tracing some laterally extensive sandstone beds.

4.2. Magnetostratigraphy

In total, from the Kvabebi section, 39 samples were selected for thermal demagnetisation (th) and 80 samples for alternating field (af) demagnetisation measurements. In addition, we also re-measured 32 doublet samples from the previously published sampling set of Agustí et al., 2009. From the Kushkuna section, 37 samples were demagnetised thermally, and 24 samples by alternating fields. All measurements have been performed in the Paleomagnetic laboratory "Fort Hoofddijk", Utrecht, following the methodology of Lazarev et al. (2019). Interpretation of the data has be done using an online platform Paleomagnetism.org (Koymans et al., 2016). This portal can be used to upload and check the paleomagnetic data, presented in this paper (Supplementary 3–4).

4.3. $^{40}Ar/^{39}Ar$ isotope dating

Three volcanic ash layers have been sampled in the field, one from the base of the Kvabebi section (KVB-1, ash 2, 129 m, Supplementary 1) and two ash layers from the Hajigabul section in the eastern Kura Basin: HG-4 (194.5 m) and HG-1033 (1030 m) (Fig. 8 in Lazarev et al., 2019). Minerals from these ash layers were separated using standard mineral separation procedures. After crushing and washing the samples, heavy liquid mineral separation with densities of 2.54 and 2.59 g/cm^3 was performed to obtain the sanidine phenocrysts from the samples. For KVB-1 also biotite was separated. Mineral fractions were further purified by hand-picking under an optical microscope. The selected mineral separates were packed in 6 mm ID AI packages. They were loaded together with Fish Canyon Tuff sanidine (FCs) standards in 25 mm ID Al cups. Samples and standards were irradiated at the Oregon State University TRIGA reactor in the cadmium shielded CLOCIT facility for 12.6 h (irradiation code VU117; equivalent to 7 h of CLICIT position). After irradiation, samples and standards were unpacked and loaded in a 185-hole Cu tray and baked overnight at 250 °C under vacuum. This tray is then placed in a doubly pumped vacuum chamber with Zn—Se window and baked overnight at 120 °C under high vacuum. This chamber is connected to a ThermoFisher NGPrep gas purification line equipped with a hot GP50, a cold finger (Lauda at −70 °C) and hot St707 getter.

Samples and standards were measured in two different trays (19 T13; 19 T14). We exposed the feldspar phenocrysts to a diffuse laser beam under UHV conditions to drive off surficial gasses in the first tray. The released gas during this pre-heating steps was not measured, but based on previous tests should not contain >1% of the $^{39}Ar_K$ released. Samples and standards are fused using a 25 W Synrad CO_2 laser. The released gas is analysed on an ARGUS VI+ noble gas mass spectrometer at the Vrije Universiteit Amsterdam. This is a high sensitivity, relatively low resolution multi-collector noble gas mass spectrometer with an internal volume of 710 ml. The resolution of the system is ~200 and, therefore, does not resolve hydrocarbon or chlorine interferences. The mass spectrometer is equipped with four Faraday cups at the H2, H1, AX, and L1 positions and two compact discrete dynodes (CDDs) at L2 and L3 positions. The system is equipped with a 10^{12} Ohm amplifier on H2 and

10^{13} Ohm amplifiers on H1, AX and L1 cups. Samples were run on H1-L3 collectors. Similar to Phillips and Matchan (2013), we did not apply bias corrections but analysed samples and standards in the same tray (and thus at more or less the same time), alternating with air pipettes with intensities in the same range as the samples and standards. Line blanks were measured every 2–3 unknowns and were subtracted from succeeding sample data.

Data reduction is made in ArArCalc (Koppers, 2002). Ages are calculated with (Min et al., 2000) decay constants and 28.201 Ma for FCs (Kuiper et al., 2008). The atmospheric $^{40}Ar/^{36}Ar$ air value of 298.56 is used (Lee et al., 2006). The correction factors for neutron interference reactions are $(2.64 \pm 0.02)\ x10^{-4}$ for $(^{36}Ar/^{37}Ar)_{Ca}$, $(6.73 \pm 0.04)\ x10^{-4}$ for $(^{39}Ar/^{37}Ar)_{Ca}$, $(1.21 \pm 0.003)\ x10^{-2}$ for $(^{38}Ar/^{39}Ar)_{K}$ and $(8.6 \pm 0.7)\ x10^{-4}$ for $(^{40}Ar/^{39}Ar)_{K}$. All errors are quoted at the 1σ level. All relevant analytical data for age calculations can be found in the appendix (Supplementary 5).

5. Results

5.1. Magnetostratigraphy of the Kvabebi section

Demagnetisation of 151 samples from Kvabebi reveals the presence of two magnetic components. The first magnetic component is a low-temperature / low-intensity component that is exclusively of normal polarity. This component is observed in 53% (51 out of 93) of the alternating field (af) demagnetisation diagrams where it ranges between 0 and 25 mT, and in 25% (14 out of 55) of the thermally demagnetised samples (th) in a temperature range of 20–270 °C (Fig. 3A). The mean directions for both low temperature (LTC) and low intensity (AF_1) groups are statistically indistinguishable and are consequently combined in one common "1st component" group (Fig. 3B). The mean direction of this component in geographic coordinates has parameters of D = 7.4°, I = 60°, k = 13.1°, α95 = 4.5° for N = 34 and D = 359.5°, I = 43.3°, k = 8.6°, α95 = 8.9° for N = 43 in tectonic coordinates (Fig. 3B).

The second magnetic component unblocks at a maximum temperature of 600 °C in th-diagrams and at 100 mT in af-diagrams (Fig. 3A). It is uniformly present in most of the studied samples and has both normal and reversed polarities (Fig. 3A, C). Thermomagnetic runs show concave or slightly convex curves that indicate a gradual decay to 600 °C (Fig. 3H). Such behaviour is characteristic of magnetite that has a Curie temperature of 580 °C, which is thus considered to be the primary magnetic carrier in the Kvabebi samples.

The mean directions acquired with both af- and th-techniques are statistically indistinguishable and are combined into "all normal" (Fig. 3D) and "all reversed" groups (Fig. 3E). The mean direction for the "all normal" group in tectonic coordinates has parameters of D = 3.5°, I = 40.3°, k = 10.4°, α95 = 4.7° for N = 96 and for the "all reversed" group these are D = 202.5°, I = −29.6°, k = 11.3°, α95 = 10.8° for N = 18 (Fig. 3D, E).

The mean directions of the "1st component" and the "all normal" component have very similar declination and inclination values in both geographic and tectonic coordinates (Fig. 3F). The bootstrap test (Tauxe, 2010) shows that the two groups fall within the 95% confidence interval and are statistically indistinguishable. Thereby, the two magnetic components may either represent a primary characteristic remanent magnetisation (ChRM) and/or a secondary viscous present-day overprint. Most strata in Kvabebi have a dip direction of 350–0° NNW with a tilt of 25° indicating that inclination values can be used to distinguish between potential magnetic overprint and ChRM directions.

The expected inclination for the Kvabebi location is I = 66.5° according to the geocentric axial dipole (GAD) for this latitude, which is nearly identical to the inclination of both groups in geographic coordinates. The inclination of both groups in tectonically corrected coordinates is too shallow compared to the expected inclination. To test for potential inclination shallowing, we applied the elongation/inclination (E/I) test of Tauxe and Kent (2004) that fits observed inclinations to the TK03.GAD Field Model using the flattening function of King (1955). The bootstrap test used in the E/I method shows an average unflattened mean inclination of 49.68° for the "all normal" group (Fig. 3G), while the application of this method to the "1st component" group did not find intersections with the TK03.GAD polynomial (negative test). Application of this method to the "all reversed" group also revealed an inclination shallowing of about 10°. Still, considering the small number of samples (19 against 80 recommended for the test), these results remain quite speculative. The E/I method shows that high-temperature/high-intensity groups "all reversed" and "all normal" underwent significant inclination shallowing. After the inclination test, these groups can be distinguished from the "1st component", and thus, we interpreted them as primary directions. The reversal test of McFadden and McElhinny (1990) applied for both "all reversed" and "all normal" groups is negative. This might be caused by the interference of primary and secondary components as well as by a small number of reversed samples. The low-temperature/low-intensity directions of the "1st component" group show no sign of inclination shallowing and are interpreted as viscous overprints.

Plotting all results in stratigraphic order reveals only two polarities; the lower part (0–210 m) is of normal polarity (N1), the upper part (210–260 m) shows reversed polarities (R1) (Fig. 4). Samples from a parallel transect (Log B) display only normal polarity directions (Supplementary 1). Measurements of doublets from the study of (Agustí et al., 2009) (Log C, Supplementary 1) also reveal only normal polarity.

5.2. Magnetostratigraphy of the Kushkuna section

Demagnetisation of 61 samples from the Kushkuna section using thermal (th) and alternating field (af) demagnetisation also shows two magnetic components. In th-samples, the first component is again a low-temperature component in the temperature range 20–270 °C. It is present in 80% of all thermally demagnetised samples (Fig. 5A). In af-samples, the first component represents low-intensity components developed in the range 0–20 mT and is present in 60% of all samples (Fig. 5A). Combining directional data of both th and af samples into a unified "1st component" group yields a mean direction of D = 0.7°, I = 65°, k = 17.5°, α95 = 7.83° for N = 21 in geographic coordinates (Fig. 5B). The expected inclination for the Kushkuna area is I = 66.5°. We, therefore, interpret the first magnetic component in the Kushkuna section as a viscous overprint as well.

The second component displays both normal and reversed polarities and demagnetises in a temperature range 290–580 °C in th-samples and 20–80 mT in af-samples (Fig. 5A, C). The bootstrap test shows that the mean directions for th- and af-samples overlap within 95% confidence interval and they were combined into two groups: "all reversed" and "all normal". The mean direction for "all reversed" in tectonic coordinates has parameters of D = 188.4°, I = −41.5°, k = 11.7°, α95 = 10.9 for N = 17 (Fig. 5D) and for "all_normal" D = 5.4°, I = 58.4°, k = 29.1°, α95 = 4.9° for N = 31 (Fig. 5E).

The acquired inclination values of −41.4° and 58.4° are again significantly shallower than the expected I = 66.5° of the geocentric axial dipole (GAD) for this area. Unfortunately, the small number of samples do not allow the application of the E/I shallowing inclination test. The reversal test of McFadden and McElhinny (1990) applied for these groups is positive. Thus, the high-temperature/high-intensity magnetic component is interpreted as characteristic for the sedimentation age (ChRM).

The magnetostratigraphic patterns of the Kushkuna section consist of one normal polarity zone (N1, 60–201 m) and one reversed zone (R1, 223–300 m) separated by a short interval of undetermined polarity (201–223 m, Fig. 4).

5.3. $^{40}Ar/^{39}Ar$ dating

For KVB-1, we analysed both the sanidine and biotite fractions. In

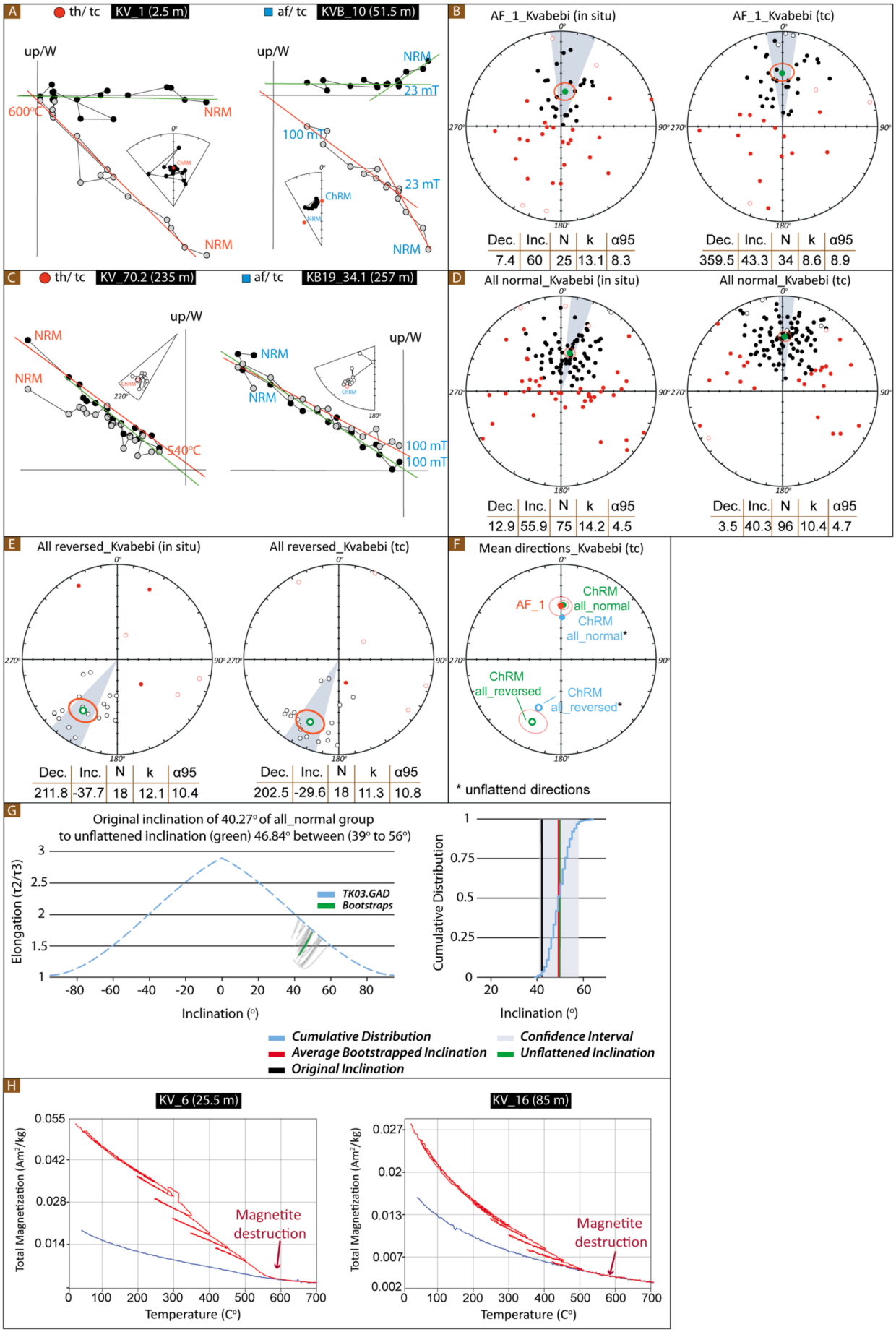

(caption on next page)

Fig. 3. Zijderveld diagrams, equal area plots, and thermomagnetic curves for samples of the Kvabebi section. Zijderveld diagrams for: A. normal samples, C. reversed samples. Equal are plots of the: B. Low-intensity 1st component; D. "All normal" (high temperature and high-intensity components); E. "All reversed" (high-temperature and high-intensity components). F. Mean directions of all determined magnetic components; G. Bootstrap test curve showing the inclination shallowing in "All normal" group; H. Thermomagnetic run curves with magnetite being interpreted as the main magnetic carrier. Abbreviations: in situ – geographic coordinates; tc – tectonically corrected coordinates, NRM – Natural remanent magnetisation, ChRM – Characteristic remanent magnetisation, Dec. – declination, Inc. – inclination, N – number of statistically accepted samples, k – precision parameter of Fisher (1953), α95–95% cone of confidence.

tray 19 T13, we fused 5 grains/hole and in tray 19 T14 7–10 grains/hole for the biotite and 5 grains/hole, respectively, for the sanidine in tray 19 T13. The average radiogenic ^{40}Ar yield for biotite is ~40% (irrespective if samples were pre-heated in UHV, or not). Ages range from 2.97 to 2.76 Ma. If we select the weighted mean age including the highest number of analyses with overlapping ages and MSWD < *t*-test statistics at 95% confidence level, the weighted mean age arrives at 2.864 ± 0.03 Ma (Fig. 6). The atmospheric $^{40}Ar/^{36}Ar$ inverse isochron intercept is 298.1 ± 2.4. Note that slightly different age interpretations are possible. Further, the relatively low radiogenic ^{40}Ar yields suggest some alteration, and thus, some minor Ar loss possibly took place, potentially leading to an underestimation of the age.

The dated feldspar fraction has low K/Ca ration (<0.1) and is, therefore, not a sanidine fraction, but rather plagioclase. Due to the low amount of K, measured intensities are low and reliable analyses would require >25 grains per fusion. The current ages already range from 66 to 2 Ma and large multi-grain experiments will be compromised by these older components. We therefore, did not attempt any further analyses. The weighted mean age of the five youngest grains is 2.55 ± 0.16 Ma, but the error is large (Fig. 6).

For HG-4 we analysed the sanidine fraction. In tray 19 T13 we fused 5 grains/hole and in tray 19 T14 15 grains/hole. Radiogenic ^{40}Ar yields for the sanidine range from 75 to 95%. If we select the weighted mean age including the highest number of analyses with overlapping ages and MSWD < t-test statistic at 95% confidence level, the weighted mean age arrives at 2.66 ± 0.05 Ma. The atmospheric $^{40}Ar/^{36}Ar$ inverse isochron intercept is 295.4 ± 4.5 (Fig. 6).

For HG-1033, we analysed the sanidine fraction. In tray 19 T13, we fused 5 grains/hole and in tray 19 T14 10 grains/hole. In both trays, we observe a large spread of ages ranging from 1.8 to 27 Ma. We conclude that this ash contains many reworked components, and reliable age information cannot be obtained from the full spectrum of data. We note, however, that the two youngest fusions yield a weighted mean age of 1.88 ± 0.03 Ma (Fig. 6).

6. Discussion

6.1. Correlation of new data to the GPTS

In both Kvabebi and Kushkuna sections, the Akchagylian starts within a long normal polarity chron. Our high-resolution magnetostratigraphic resampling of the Kvabebi section did not confirm the presence of a short reversed polarity interval at the stratigraphic succession (140–160 m of Kvabebi log in Fig. 4, Supplementary 1) that comprises the mammalian fossil site (Agustí et al., 2009). We did detect several weakly magnetised samples that may explain a different (reversed polarity) interpretation. However, placing strict criteria on the demagnetisation results leads us to conclude that the Kvabebi magnetostratigraphy comprises a single normal polarity interval from the base of the section until the transition to reversed polarities at level 210 m (Fig. 4). This is in good agreement with the magnetostratigraphic results of the Kushkuna section that also reveals a long (~150 m) normal polarity interval at the lower part of the section. The $^{40}Ar/^{39}Ar$ dating of the volcanic ash 2 at Kvabebi (129 m) resulted in two different ages: a high-uncertainty feldspar-based age of 2.55 ± 0.16 Ma and a more reliable biotite-based age of 2.86 ± 0.03 Ma (Fig. 6). Both ages support the correlation of the normal polarity interval to the upper Gauss chron (C2An.1n) (Fig. 7A).

Our new $^{40}Ar/^{39}Ar$ ages from the Hajigabul section confirm the previous magnetostratigraphic correlation to the GPTS by Lazarev et al. (2019). Ash layer HG-4, which is located at the Productive Series–Akchagylian transition, has an $^{40}Ar/^{39}Ar$ age of 2.66 ± 0.05 Ma (Fig. 6). It indicates that the normal to reversed polarity transition at the base of the Akchagylian stage indeed correlates to the Gauss–Matuyama (C2An.1n/C2r.2r) boundary (2.61 Ma; Raffi et al., 2020). The two youngest dates for ash layer HG-1033 at level 1012 m yield 1.88 ± 0.03 Ma. This level is positioned within a normal polarity interval that was correlated to the Olduvai chron (C2n; 1.95–1.77 Ma) by Lazarev et al. (2019). This new $^{40}Ar/^{39}Ar$ age therefore validates the correlation of the normal polarity interval below the Olduvai, straddling the Akchagylian–Apsheronian transition to the Reunion subchron (C2r.1n: 2.14–2.12 Ma).

In summary, all three sections – Kvabebi, Kushkuna and Hajigabul validate the base of the Akchagylian to occur within the upper Gauss chron and in Hajigabul, the Akchagylian-Apsheronian transition correlates to the Reunion subchron (Fig. 7A).

6.2. Akchagylian age constraints and chronostratigraphic correlations in the Kura Basin

The Akchagylian deposits in the Kura Basin have been extensively studied in the last decade using a combination of magneto- and biostratigraphy and $^{40}Ar/^{39}Ar$ isotopic dating. In the Jeirankechmez, Babazanan and Hajigabul sections located in the eastern and central Kura Basin, the onset of the Akchagylian has been defined as an influx of new brackish water (meso- to euhaline) faunas (including ostracods, foraminifera and molluscs) that occurred at ~2.7 Ma within the upper Gauss chron (van Baak, 2015; Richards et al., 2018; Lazarev et al., 2019; van Baak et al., 2019). The base of the Akchagylian has been correlated here to the Akchagylian marine incursion – the onset of the Caspian-Arctic interbasinal connectivity (van Baak, 2015). However, no universally agreed age estimates have been determined on the age of the Akchagylian transgression that precedes the marine incursion in all studied sections.

The chronology and hydrological history of the lowermost Akchagylian have recently been re-investigated in the Lokbatan section, in the interval 520–541 m (Fig. 7B). Application of high-resolution palynology and dinocyst analyses accompanied by $^{40}Ar/^{39}Ar$ dating of several volcanic ashes showed that the pollen assemblage zones (PAZ) in the interval 528–541 m correlate to Marine Isotope Stages (MIS) between 2.86 and 2.45 Ma (Hoyle et al., 2020). The Akchagylian marine incursion, characterised by an abrupt dinocyst change from brackish water *Impagidinium*-related forms to marine *Operculodinium* at 529 m, correlates to MIS G7, dated at 2.75 Ma (Hoyle et al., 2021). The interval between the Akchagylian transgression (520 m) and the Akchagylian marine incursion (529 m) is older than 2.78 Ma but could not be adequately age-calibrated due to the poor preservation of palynological material. The calculation of average sedimentation rates within the calibrated part (528–541 m) of the Lokbatan section results in a rate of 0.04 m/kyr. Downward extrapolation of this rate to the interval with offshore claystones (520–528 m) results in an age of ~2.97 Ma for the Akchagylian transgression (Fig. 7B).

Magnetostratigraphic patterns in Jeirankechmez and Babazanan (van Baak, 2015; van Baak et al., 2019) covering the entire Gauss chron (upper Productive Series – Akchagylian) also provide a great possibility for dating the Akchagylian transgression. In both sections, brown

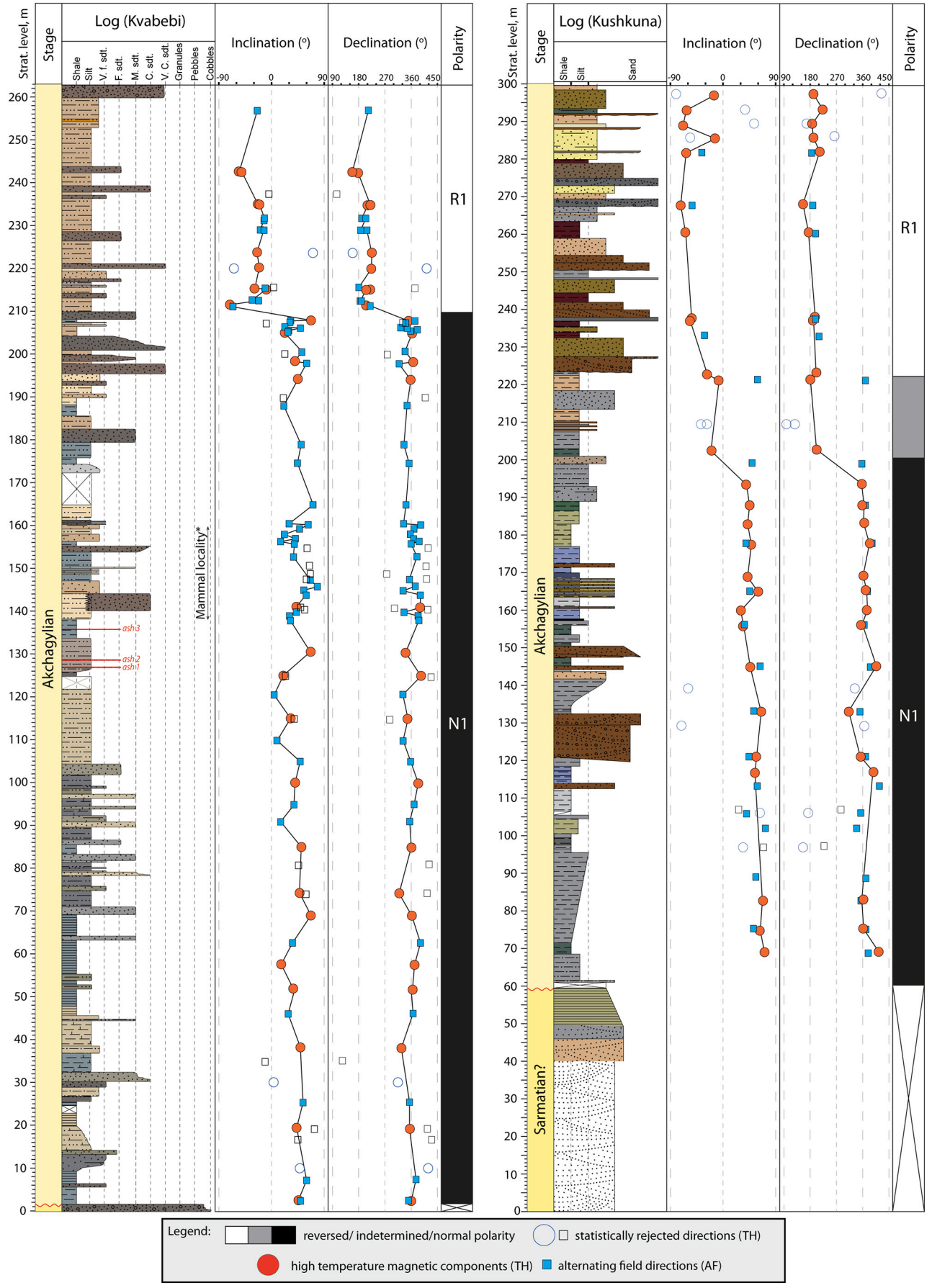

Fig. 4. Composite sedimentary logs and magnetostratigraphy of the Kvabebi (left) and Kushkuna (right) sections.

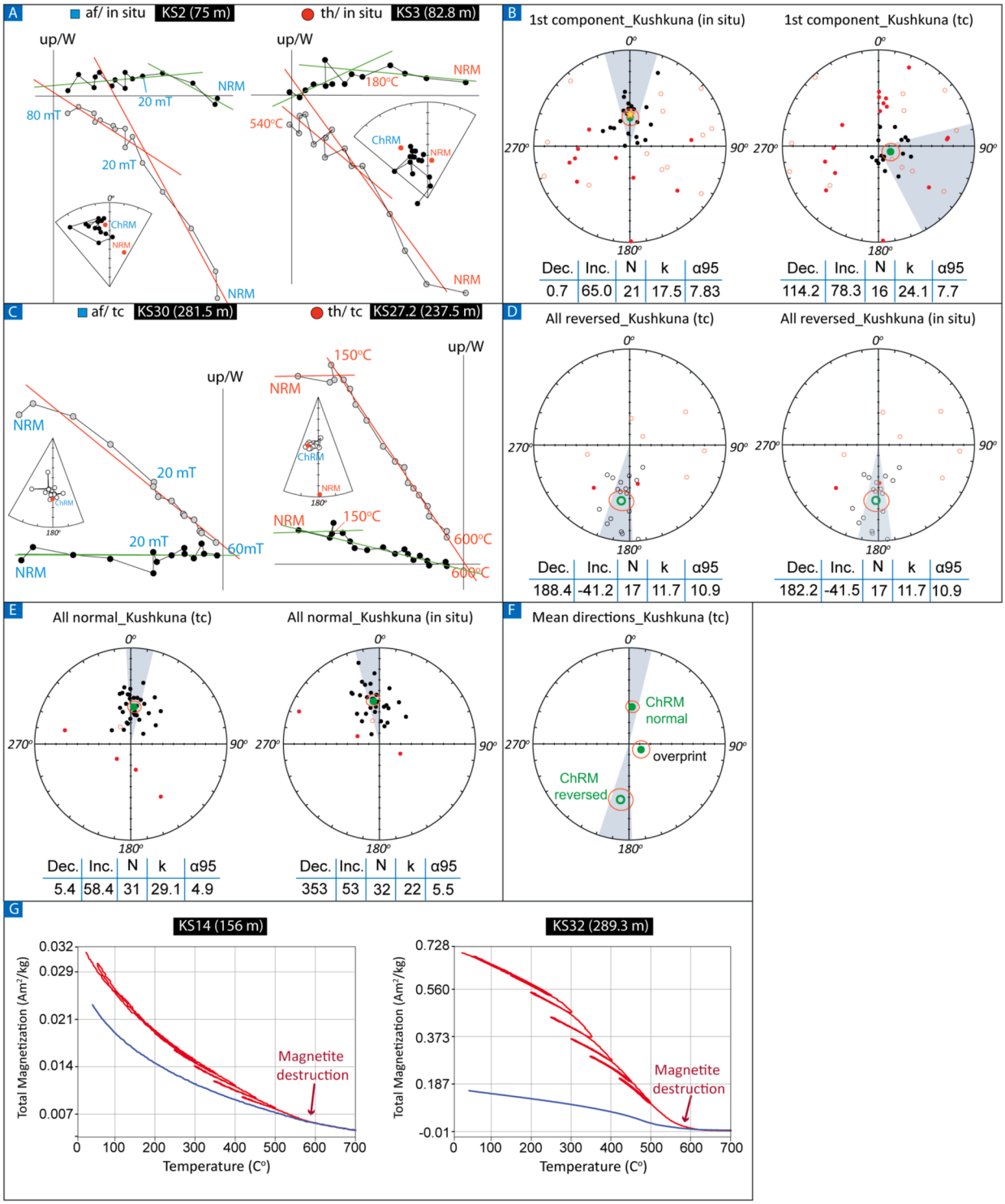

Fig. 5. Zijderveld diagrams, equal area plots, and thermomagnetic curves for samples of the Kushkuna section. Zijderveld diagrams for: A. normal samples, C. reversed samples. Equal area plots of the: B. 1st component (combined low temperature and low intensity); D. All reversed (high-temperature and high-intensity components); E. All normal (high-temperature and high-intensity components). F. Mean directions of all determined magnetic components; G. Thermomagnetic run curves with magnetite being interpreted as the main magnetic carrier. Abbreviations are given on Fig. 3.

fluvial-deltaic siltstones, mudstones and sandstones of the Productive Series are followed by grey, relatively deep-water Akchagylian claystones. In Jeirankechmez, the average sedimentation rate within the Kaena subchron is 1.38 m/kyr. Extrapolation of this rate on the lithologically-similar upper Gauss part leads to an age of 2.93 Ma for the Akchagylian transgression. The same age has been acquired by extrapolation of the 0.77 m/kyr rate derived from the Kaena–upper Gauss interval in the Babazanan section (Fig. 7C).

The results from all these sections are in good agreement and indicate that the Akchagylian transgression occurred between 2.97 and 2.93 Ma. The comparison of age constraints and lithological patterns suggests a strong drop in average sedimentation rates from 1.38–0.77 m/kyr in the fluvial-deltaic deposits of the upper Productive Series to 0.04–0.05 m/kyr in the offshore claystones of the lowermost Akchagylian. Such

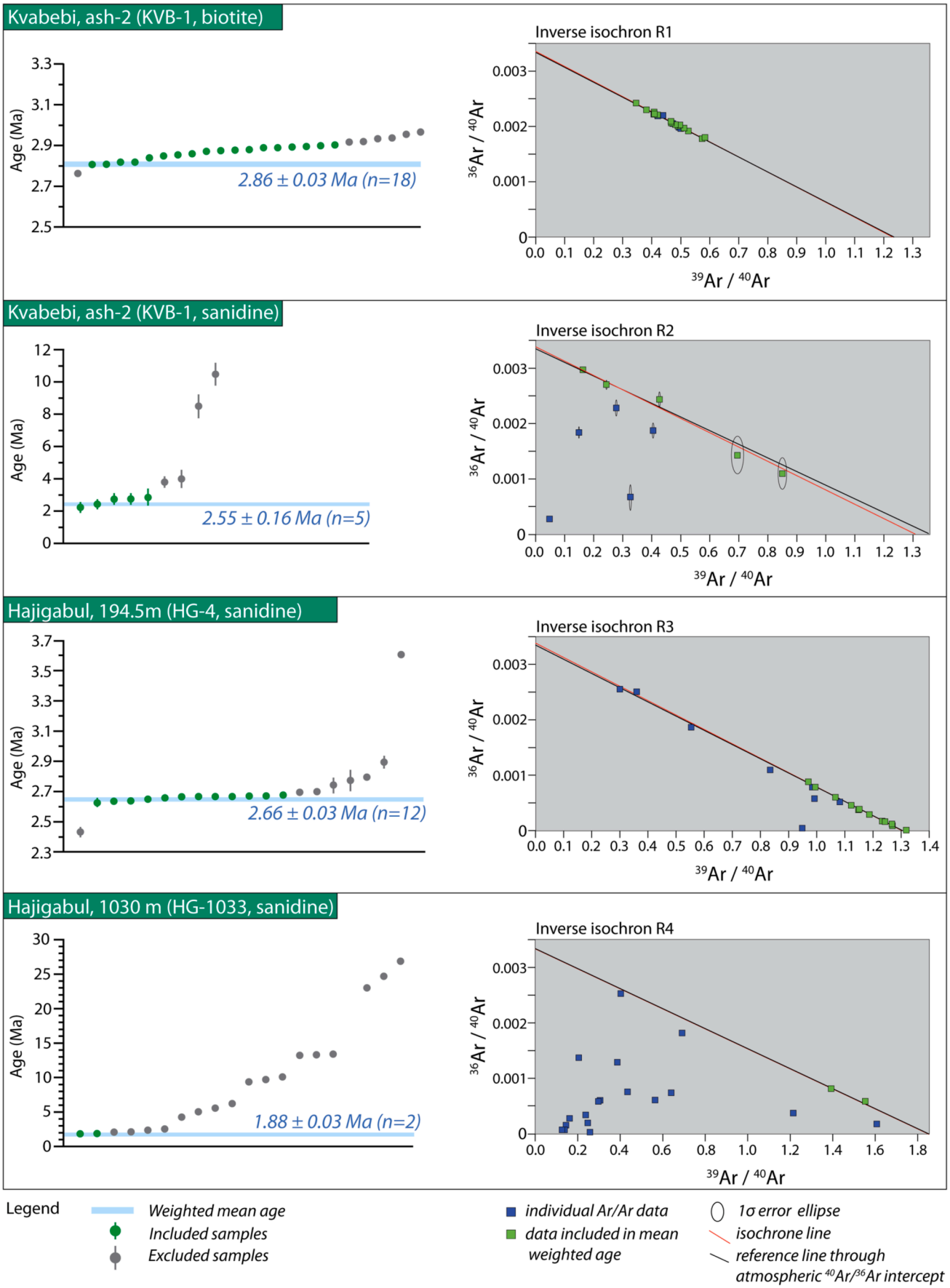

Fig. 6. $^{40}Ar/^{39}Ar$ ages with error bars for selected biotite and sanidine grain sets from volcanic ash samples and corresponding inverse isochrones. Stratigraphic levels for samples from Hajigabul are in Lazarev et al. (2019).

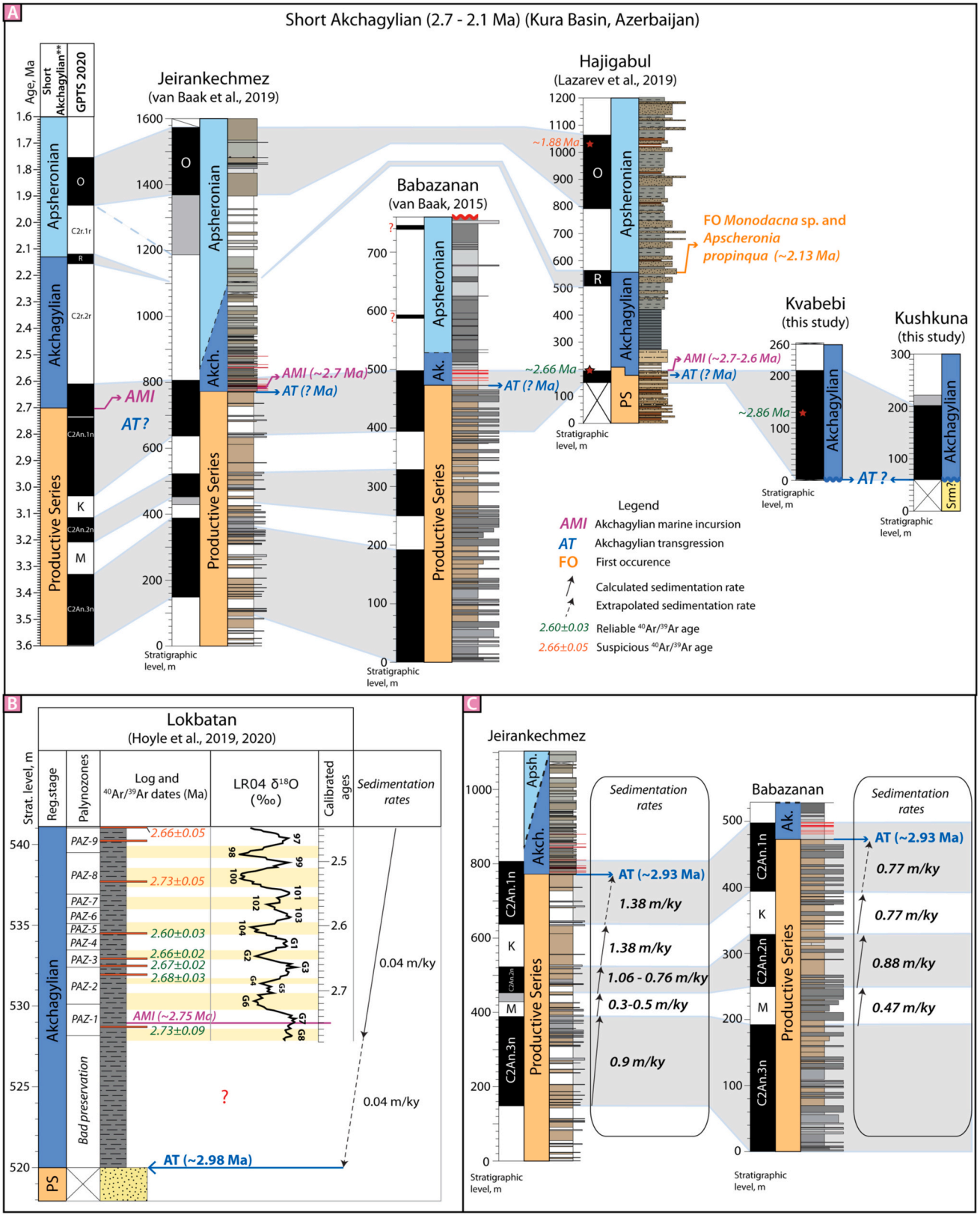

Fig. 7. Revision of the "short Akchagylian" age model. A. Magnetostratigraphic correlation of the key-sections in the Kura Basin: Jeirankechmez (van Baak et al., 2019), Babazanan (van Baak, 2015) and Hajigabul (Lazarev et al., 2019) and Kushkuna and Kvabebi (this study) to GPTS 2020 (Raffi et al., 2020). Magneto-stratigraphy and $^{40}Ar/^{39}Ar$ dating from Kvabebi suggests earlier onset of the Akchagylian than 2.7 Ma. B. Calibrated chronology of the Lokbatan section based on high-resolution palynological analysis correlated to MIS Stages (Hoyle, 2019; Hoyle et al., 2020). Extrapolation of sedimentation rates from calibrated part of the section downwards results in the age of the Akchagylian transgression ~2.97 Ma. C. Sedimentation rates within the Productive Series in the Jeirankechmez and Babazanan sections. Extrapolation of sedimentation rates from Kaena subchron to the Productive Series part of the upper Gauss results in the age of the Akchagylian transgression at ~2.93 Ma.

change is somewhat unusual but not impossible, considering landward retreat of the major sediment-supply sources during rising sea-level (e.g. Transgressive Systems Tract) (Catuneanu et al., 2009). The 2.93–2.97 Ma age (2.95 ± 0.02 Ma) of the Akchagylian transgression implies that the lower boundary of the Akchagylian stage falls within the upper Gauss chron (C2A.1n).

The first occurrence of indicative Apsheronian molluscs falls within the first normal subchron after the Gauss-Matuyama reversal, as revealed in the Duzdag and Hajigabul sections of the Kura Basin. In Duzdag, this normal zone was first correlated to the Olduvai (Pevzner, 1986), but later a correlation to the Reunion subchron was proposed (Krijgsman et al., 2019). In Hajigabul, the correlation to Reunion subchron was established based on the position between two normal chrons interpreted as upper Gauss and Olduvai (Lazarev et al., 2019) whose correlation is now supported by our new $^{40}Ar/^{39}Ar$ constraints. We thus conclude that the Akchagylian-Apsheronian boundary correlates to the Reunion subchron and has an age of ~2.13 Ma.

6.3. Akchagylian age constraints and correlation in Kopet-Dag and Turkmenian shore

The "long Akchagylian" age model was developed based on the extensive palaeomagnetic study of Akchagylian deposits on the Turkmenian side of the Caspian Sea in the 1970's (Trubikhin, 1977). Here, palaeomagnetic studies of 20 sections generally found the Akchagylian erosively overlying the continental Toronglinsk Suite/Red Colour Formation within the long normal polarity interval of the Gauss chron, that changes higher up to a long reversed interval (Fig. 8A). This reversal was thus interpreted as the Gauss-Matuyama reversal, dated back then at 2.44 Ma (Cox, 1969). In 8 out of 20 sections (i.e. Gokchadere, Issu, Kushuldzha, Orumeldzha, Diodzhi, Pyrnuar, Zau and Khalats) one or two small magnetic reversals were revealed within the Gauss chron, interpreted as the Kaena and Mammoth subchrons (Trubikhin, 1977). The base of the Akchagylian was then correlated to the base of the Gauss Chron (Fig. 9A) and in its current age of 3.6 Ma is nowadays used in the Russian stratigraphic chart of the Caspian region (Zastrozhnov et al., 2013).

The original out-of-scale representation of the short reversed intervals on Fig. 30 in Trubikhin (1977), may lead to a univocal conclusion that they represent the Kaena and Mammoth subchrons. However, the simple on-scale redrawing of this data clearly demonstrates that these reversed intervals are far too short (Fig. 8). In Gockhadere, Issu, Kushuldzha and Khalats, only one small reversed zone was found within the Gauss; in Orumeldzha and Diodzhi two intervals with uncertain polarity were revealed and only in Pyrnuar and Zau two short reversed zones were detected (Fig. 8). The magnetostratigraphy of the Zau section was later revised, showing only one small reversed zone, but the correlation to the Mammoth or Kaena remained (Vardanyan et al., 2003).

The calculation of sedimentation rates within the potential Kaena and Mammoth subchrons demonstrates a nine times decrease compared to the normal subchrons directly below and above (Fig. 8B). Such change is not impossible as we previously calculated for the Productive Series – Akchagylian boundary in the Kura Basin. However, in the Kura Basin, the drop in sedimentation rates is attributed to a change in depositional environments from deltaic sandstones and mudstone of Productive Series to low-energy deep-water claystone of Akchagylian. The Pyrnuar section, on the contrary, demonstrates a clear lithological coarsening trend to sandstones, which is likely reflective of an sedimentation rate increase (Fig. 8B). Unreasonably small thickness of reversed intervals and the drop in sedimentation rates are thus not in agreement with the observed lithological trends.

A recent reassessment of the Pyrnuar magnetostratigraphy also concluded that the two reversed intervals are too short to be correlated to Kaena and Mammoth (Gurarii, 2015). The reversed directions were then reinterpreted as magnetic excursions, and the base of the Akchagylian was correlated to the base of the upper Gauss chron (C2An.1n) (Gurarii, 2015). In our opinion, the small reversal excursion within the upper Gauss chron may potentially correlate to the Porcupine excursion dated ~2.74 Ma (Channell et al., 2016), although reassessment of the magnetic signal (magnetic mineral carriers and intensity) is highly required.

We conclude that in none of the eight sections (i.e. Gokchadere, Issu, Kushuldzha, Orumeldzha, Diodzhi, Pyrnuar, Zau and Khalats) the short reversed intervals in the Akchagylian are unambiguously correlated to the Kaena and Mammoth subchrons. We consider it more likely that the observed short reversed intervals correspond to excursions of the magnetic field. This leads to a conclusion that in sections on both the western (Kura Basin) and eastern (Turkmenistan) coasts of the Caspian Sea, the onset of the Akchagylian (Akchagylian transgression) correlates to the upper Gauss chron (C2An.1n).

The biggest confusion over the magnetostratigraphic correlation of the Akchagylian-Apsheronian boundary occurred due to ongoing improvements of magnetostratigraphic methodology and refinement of the GPTS, especially in the last decades (Langereis et al., 2010). The most noticeable changes occurred within the late Pliocene – Pleistocene magnetostratigraphy. Since Cox (1969), the long Gilsa subchron transformed into the long Olduvai subchron, and two original Olduvai subchrons are now merged into one Reunion subchron (Figs. 7B, 8A).

6.4. Palaeoenvironmental and palaeogeographic reconstructions of the Caspian Basin during the Akchagylian

6.4.1. From Akchagylian transgression to Arctic connection (~2.95–2.75 Ma)

Our new and revised paleomagnetic and $^{40}Ar/^{39}Ar$ data show that the early Pliocene lowstand of the Caspian Sea was terminated by the Akchagylian transgression at ~2.95 ± 0.02 Ma. The major lithological change traced throughout the Kura Basin, suggests that depositional settings changed drastically from terrestrial/fluvial-deltaic in the Productive Series to offshore and nearshore environments in the Akchagylian (Fig. 9) (Vincent et al., 2010; Lazarev et al., 2019; Jorissen, 2020). In the Jeirankechmez and Lokbatan sections, the post-transgressive interval (2.95–2.75 Ma) comprises poorly-preserved faunal assemblages with reworked foraminiferal assemblages (Richards et al., 2018), freshwater algae *Pediastrum* and fresh-brackish water dinocysts *Komewuia*? sp. and *Impagidinium* sp. (DAZ-1) (Hoyle et al., 2021) In Kvabebi and Kushkuna, a scarce mollusc fauna with taxa like *Cerastoderma dombra* and *Avimactra subcaspia* was found (Djikia, 1968; Lebedeva, 1972). In the Fore-Ural region (North Caspian), the stratigraphic position of the lowermost Akchagylian remains unclear due to a poor fossil record complicated by strong freshening of the North Caspian Basin. Among potential stratigraphic analogues is the Kumurly horizon that spans the upper Gauss chron (Yakhimovich and Suleymanova, 1981; Zastrozhnov et al., 2021). However, a proper chronostratigraphic correlation there requires better dating, biostratigraphy and sedimentology.

The revised ages for the Akchagylian transgression and the Akchagylian marine incursion influence our understanding on the mechanism of the Caspian Sea refill. The expansion of the Caspian Sea during the Akchagylian has been assumed to be caused by either an increase of regional fresh water input (concept of positive water budget) or through a connection to another water body (flooding concept) (Krijgsman et al., 2019). The flooding concept through a connection with the Arctic Ocean (Akchagylian marine incursion) has been actively advocated in the Kura Basin, as the base of the Akchagylian was correlated to the Akchagylian marine incursion dated at 2.75 Ma(Lazarev et al., 2019; van Baak et al., 2019). However, the zoom-in palynological study in the Lokbatan, Jeirankechmez and Babazanan sections showed that the interval from the Akchagylian transgression to the marine incursion contains no marine elements (Hoyle et al., 2021; Richards et al., 2021) but encloses a time interval of about 200 kyr (Fig. 7B). This observation suggests that the Caspian Sea started expanding due to the increased freshwater input,

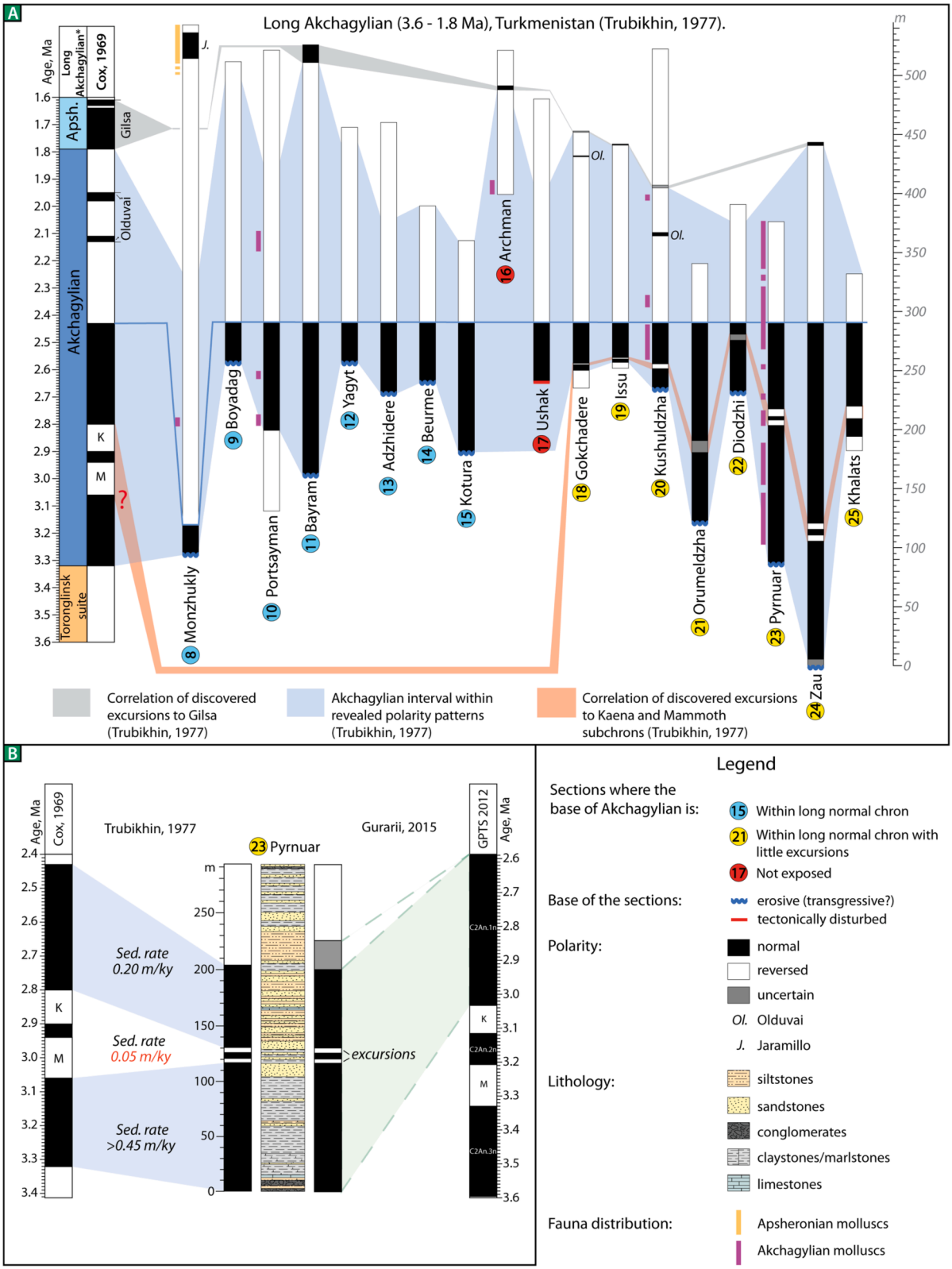

Fig. 8. Revision of the "long Akchagylian" age model. A. The on-scale redrawing of magnetostratigraphic correlation of Turkmenistan sections to GPTS of Cox (1969) after Trubikhin (1977) showing the real size of polarity intervals. B. Magnetostratigraphic correlation of polarity patterns in the Pyrnuar section made by Trubikhin (1977) (left) and its revision by Gurarii (2015) (right). Calculation of sedimentation rates was done using the GPTS 2020 (Raffi et al., 2020).

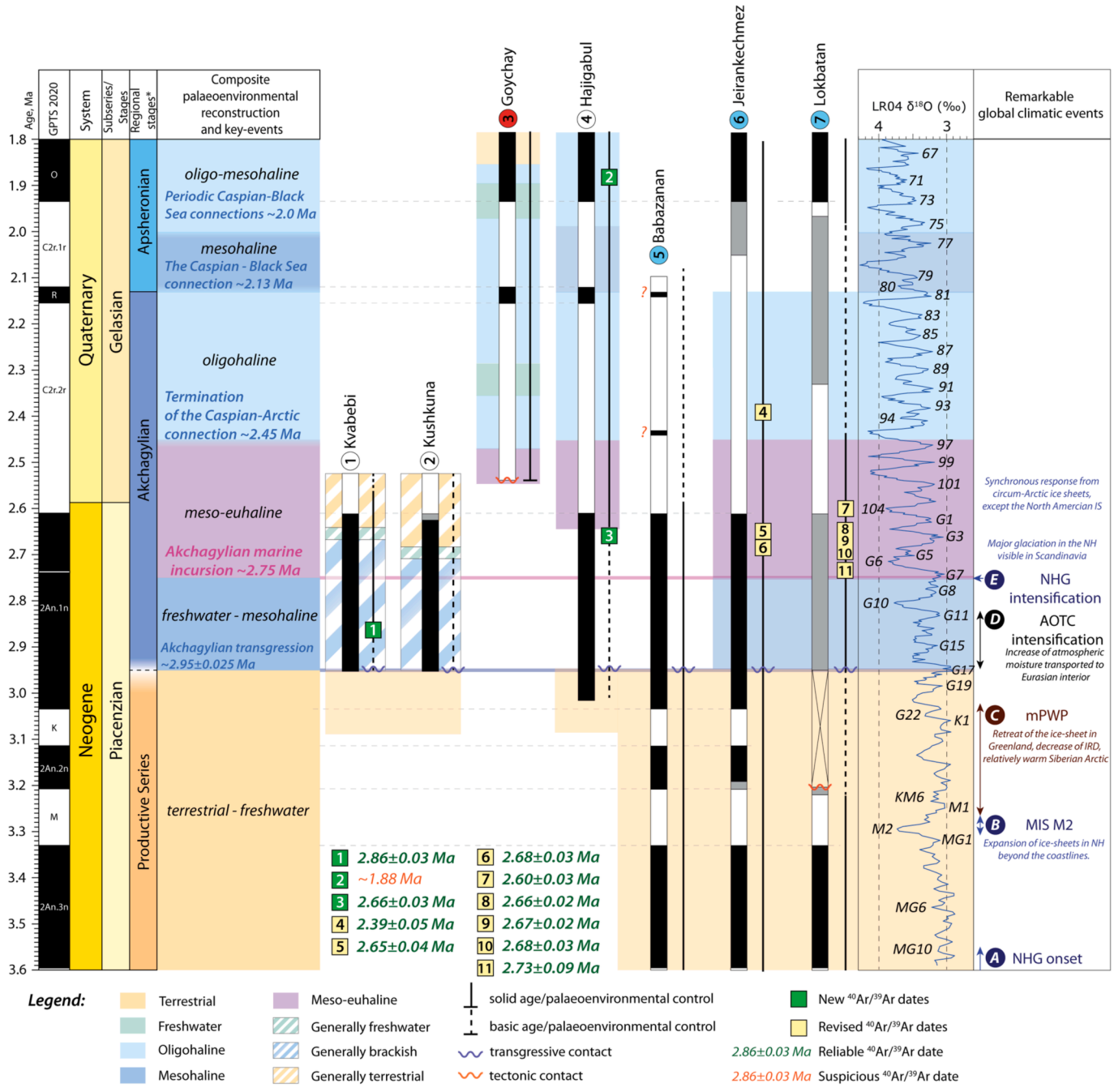

Fig. 9. Palaeoenvironmental reconstruction and unified age constraints for the Akchagylian Stage based on magnetostratigraphic, $^{40}Ar/^{39}Ar$ and biostratigraphic data from the Kura Basin. Data from presented sections (see Fig. 1 for their location) were taken from: Kvabebi and Kushkuna (this study and Jorissen, 2020), Goychay and Hajigabul (this study and Lazarev et al., 2019), Babazanan (van Baak, 2015), Jeirankechmez (Richards et al., 2018; van Baak et al., 2019), Lokbatan (van Baak, 2015; Hoyle, 2019; Hoyle et al., 2020). MIS stages curve and GPTS 2020 (Lisiecki and Raymo, 2005; Gibbard and Head, 2020; Raffi et al., 2020). Global climatic events: A – Onset of the Northern Hemisphere Glaciation (de Schepper et al., 2014); B – Marine Isotope Stage M2 (de Schepper et al., 2014); C – middle Pliocene Warm Periode (Haywood et al., 2016); D – Intensification of the Atlantic Ocean Thermohaline Circulation (Bartoli et al., 2005); E – Intensification of the Northern Hemisphere Glaciation (Lawrence et al., 2009; de Schepper et al., 2014). Acronyms: IS – Ice Sheet, IRD – Ice-rifted Debris.

which brings forward the concept of the positive water budget.

Interestingly, the North Atlantic Deep Water record demonstrates a rise of the sea surface temperature by 2 °C between 2.95 Ma and 2.82 Ma, which has been linked to the interglacial intensification of the Atlantic Thermohaline Circulation (Bartoli et al., 2005). This process potentially triggered an increase of evaporation and available moisture which via Westerlies would be transported to the Eurasian interior, in particular to Western Siberia (Driscoll and Haug, 1998). In parallel, this would also amplify precipitation over the Russian Plate increasing the freshwater runoff of the major rivers feeding the Caspian Sea – the Volga River, the Ural River etc. leading to the switch to a positive hydrological balance of the Caspian Sea.

6.4.2. *Arctic connection and "Marine "Akchagylian (~2.75–2.45 Ma)*

At 2.75 Ma, a sudden influx of meso-euhaline fauna and microflora (dinocysts) in the Caspian fossil record and the rise of the $^{87}Sr/^{86}Sr$ isotopic ratio characterise the establishment of a hydrological connection between the Caspian Sea and the global ocean (Richards et al.,

2018; Bista, 2019; Hoyle et al., 2021). Introduction of certain faunal elements into the Caspian Sea, such as foraminifera (Zubakov and Borzenkova, 1990; Richards et al., 2018), crustaceans (Väinölä, 1995) and seals (Palo and Väinölä, 2006) and dispersion of Pontocaspian faunal elements further north (Vandendorpe et al., 2019), favours a northward connection with the Arctic Ocean. The palaeomagnetic and biostratigraphic data from the Taman Peninsula (Veselovka section on the Black Sea coast) suggests that during this time, the Caspian Sea level increased and overspilled into the neighbouring Azov Sea (Taman layers) (Zubakov, 2001), and potentially connected with the Black Sea and perhaps even with the Aegean (Zubakov and Borzenkova, 1990; Taner, 1997; Krijgsman et al., 2020).

During the "marine" Akchagylian, the marginal sections of the Kura Basin (i.e. Kvabebi, Kushkuna), Turkmenistan coast (i.e. Pyrnuar, Kushuldzha, Monzhukly, Portsayman) and the North Caspian (i.e. Akkulayevo and Pre-Ural boreholes) comprise diverse Akchagylian mollusc fauna with indicative genera such as *Cerastoderma*, *Aktschagylia*, *Andrussovicardium*, *Miricardium* and *Avicardium*, often admixed with freshwater and terrestrial taxa (Djikia, 1968; Lebedeva, 1972; Trubikhin, 1977; Danukalova, 1996). In more distal parts of the basin (i.e. sections Hajigabul, Goychay, Jeirankechmez, Lokbatan), the mollusc fauna is rare and faunal assemblages contain rich meso-euhaline assemblages with abundant ostracods taxa *Loxoconcha* spp., *Amnicythere* spp., *Eucythere naphtatscholana*, *Tyrrhenocythere andrussovi*, *T. bailovi*, foraminiferal taxa *Ammonia* spp., *Cassidulina* spp., *Cibicides* spp. and *Elphidium* spp. and dinocyst taxa *Lingulodinium machaerophorum*, *Spiniferites*, *Impagidinium*, *Algidasphaeridium* cf. *capillatum* and *Operculodinium centrocarpum* (van Baak et al., 2013; Richards et al., 2018; Hoyle, 2019; Krijgsman et al., 2019; Lazarev et al., 2019). The latter two taxa indicate "true oceanic" salinity values up to ~35 psu (Hoyle et al., 2021).

At approximately 2.6 Ma, the marine fauna disappears in the records of Kvabebi and Kuskuna, and local depositional environments change to continental and fluvial coarse-grained facies (Fig. 9) (Jorissen, 2020). A similar regressive trend is also observed in the Vashlovani section (Central Kura Basin) and probably reflects the increase of sediment supply caused by the growth of the Greater Caucasus (Forte et al., 2015). Enhanced sediment accumulation rates expressed in the maximum thickness of the upper Gauss chron in the entire Kura Basin (Fig. 7A) may suggest that at that time, the western part of the Kura Basin underwent stronger subsidence than in the eastern part as a result of the depocenter mobility and growth strata (Alania et al., 2017).

6.4.3. Desalinated Akchagylian (2.45–2.13 Ma)

At ~2.45 Ma, marine faunal elements like dinocysts (e.g. *Operculodinium centrocarpum*), foraminifera (*Cassidulina*, *Cibicides*, *Hanzawaia*), and most molluscs disappear from the Caspian fossil record (Paramonova, 1994; Richards et al., 2018; Hoyle et al., 2021). The marginal geological records of Turkmenistan, Kura Basin (Goychay) and the North Caspian (Fore-Ural boreholes) display frequent intervals with freshwater fauna pointing at the enhanced freshening of the basin margins (Trubikhin, 1977; Yakhimovich and Suleymanova, 1981; Lazarev et al., 2019). In sections representing more distal parts of the basin (Hajigabul, Lokbatan, Jeirankechmez), the oligohaline ostracod assemblages remain relatively stable and continue into the Apsheronian Regional Stage (van Baak et al., 2013; Richards et al., 2018; Krijgsman et al., 2019; Lazarev et al., 2019). This event is accompanied by the overall decrease of Sr-isotopic ratios, indicating the termination of the Caspian-Arctic connection (Bista, 2019; van Baak et al., 2019).

At around 2.25 Ma, the lithological change from offshore mudstones to nearshore sandstones characterises the first well-pronounced lowering of the water level observed in the eastern Kura Basin (Lazarev et al., 2019). Depositional environments switched from offshore-dominated successions to well-pronounced obliquity-controlled offshore-backshore parasequences (Jorissen et al., 2019). This event potentially correlates to the regressive lithological trend in the uppermost Akchagylian reported from the North Caspian (Zubakov and Borzenkova, 1990) and Fore-Ural region (Yakhimovich and Suleymanova, 1981) but requires further solidification of the age constraints.

6.4.4. Akchagylian – Apsheronian transition (2.13–2.0 Ma)

At ~2.13 Ma, a new Apsheronian indicative mollusc fauna with *Monodacna* sp. and *Apscheronia propinqua* marks the Akchagylian-Apsheronian boundary (Lazarev et al., 2019) (Fig. 9).

The fossil mollusc fauna has been traditionally used for stratigraphic subdivision and correlation in the Paratethyan and Pontocaspian regions (Paramonova, 1994; Danukalova, 1996; Popov et al., 2010). However, due to the very limited palaeoecological distribution of molluscs, many geological sections, especially those representing the deeper environments, contain no molluscs. Drawing of strict boundaries in such sections was always challenging and provoked many discussions regarding the other potential biostratigraphic markers, like the ostracod fauna. In the Xocashen section (Kura Basin), the Akchagylian-Apsheronian boundary was placed at the level of the first occurrence of *Tyrrhenocythere donetziensis* and *T. pontica* dated there at ~2.0 Ma (van Baak et al., 2013). In the Hajigabul and Goychay sections, another ostracod species occurring at ~2.1 Ma - *Tyrrhenocythere azerbaijanica* was proposed as a potential marker (Lazarev et al., 2019). In the Jeirankechmez section, the boundary was determined by a massive occurrence of *Amnicythere* species as well as dinocysts of "Pannonian" or Black Sea affinity dated at ~2.4 Ma (Richards et al., 2018). There is as yet no consensus about what microfauna can be considered as an additional biostratigraphic marker. The high variability of depositional settings may affect the synchronicity of faunal distribution in different parts of the basin.

The Akchagylian-Apsheronian boundary in the Hajigabul section comprises changes in mollusc fauna and microfauna, all placed in a solid magnetostratigraphic age frame and now supported by $^{40}Ar/^{39}Ar$ dating. Among all applied proxies, magnetostratigraphy remains one of the most robust markers for the Akchagylian-Apsheronian boundary. At the current state of research, we propose to place the Akchagylian-Apsheronian boundary at the Reunion (Feni) subchron (C2r.1n), dated in GPTS 2020 between 2.15 and 2.12 Ma (Raffi et al., 2020).

At ~2.1 Ma in Hajigabul, a massive occurrence of mesohaline microfauna with ostracods and foraminifera was detected following the first Apsheronian molluscs (Lazarev et al., 2019). The rise of Sr-isotope ratios in Goychay at 2.1 Ma towards the Black Sea levels (Bista, 2019) suggests that the faunal influx in Hajigabul could be caused by the establishment of a Caspian-Black Sea connection. The integrated sedimentological-isotopic-faunal-climate modelling study of the lower Apsheronian interval in the Hajigabul section suggests that the Caspian Sea was repeatedly connected to the Black Sea during the obliquity-maxima intervals (Jorissen, 2020).

6.5. Implication of new age constraints for other interdisciplinary studies

The new geochronological constraints restrict the Akchagylian to the time interval between 2.95 Ma and 2.1 Ma, which is significantly shorter than in the regional geological time scales (Zastrozhnov et al., 2013). This appeals to a revision of numerous archaeological, faunal and palaeoenvironmental reconstructions in the Caspian region, where Akchagylian deposits were used as a time benchmark.

The palaeoclimate data derived from a palynological study of the Terek Basin (North Caspian Basin) shows significant warming characterised by the expansion of the broad-leaved mixed oak forests (Naidina and Richards, 2016). This event has been attributed to the lower Akchagylian and has initially been correlated to the mid-Pliocene Warm Period dated at 3.2 Ma using the "long Akchagylian" time frame. Here we proclaim that this warm interval is significantly younger, and its geochronological position is yet to be revised.

The new age constraints from Kvabebi and Kushkuna also clarify the regional stratigraphic position of mammalian fauna found therein (Ali-Zade et al., 1972; Lebedeva, 1972; Vekua, 1972). These two large

mammalian fossil faunas from the Kura margin are attributed to biozone MN16b (~2.8–2.5 Ma) (Bukhsianidze and Koiava, 2018; Krijgsman et al., 2019). These views, however, were in contradiction with the previous age model for Kvabebi site, that dated the mammal locality at 3.1 Ma (Agustí et al., 2009). The MN16b zone is, however, in good agreement with our new chronology for the western Kura Basin, which may further help to improve the biogeographic history of the region.

The Akchagylian deposits have also been widely used in the regional archaeological studies, where they serve as a good time indicator. One of the most enigmatic archaeological sites in the Caspian region is Rubas-1, located in Dagestan (Russia). In this locality, one of the oldest stone tools of Eurasia are covered by Akchagylian deposits that with the previous magnetostratigraphic age constraints have been dated between 2.2 Ma and 1.75 Ma (Derevianko et al., 2015). Our new age constraints on the Akchagylian indicate that the stone tools in the Rubas-1 should be older than 2.13 Ma.

7. Conclusion

Magnetostratigraphic and $^{40}Ar/^{39}Ar$ dating of three sections in the Kura Basin and revision of existing age constraints in 25 sections across the South Caspian region allowed resolving the major age controversies for the Akchagylian Regional Stage.

Our new high-resolution sampling of the Kvabebi section and re-measuring of the old sample set published in Agustí et al. (2009), did not confirm the presence of the Kaena subchron. Instead, we found that the Akchagylian begins as a transgression event within the long normal polarity interval that switches higher up to a reversed polarity interval. We interpret this polarity change as the Gauss-Matuyama reversal. The $^{40}Ar/^{39}Ar$ dating of volcanic ash from below the reversal resulted in an age of 2.86 ± 0.03 Ma supporting our correlation of the normal polarity interval to the upper Gauss.

Magnetostratigraphic dating of the neighbouring Kushkuna section also found the onset of the Akchagylian within the upper Gauss chron switching higher up to Matuyama. The $^{40}Ar/^{39}Ar$ dating of volcanic ashes (2.66 ± 0.03 Ma and ~ 1.88 Ma) from two normal polarity intervals in the Hajigabul section validated their previously proposed correlation to the upper Gauss and Olduvai subchrons, respectively. It also verified the correlation of the normal interval spanning the Akchagylian-Apsheronian boundary to the Reunion subchron.

Revision of five sections in the Kura Basin that supported the “short Akchagylian” model (2.7–2.1 Ma) showed that the onset of the Akchagylian Stage was correlated to the *Akchagylian marine incursion* event and no age estimates were yet obtained for the preceding *Akchagylian transgression*. Calculation of sedimentation rates in the Lokbatan, Jeirankechmez and Babazanan sections resulted in an age of 2.95 ± 0.02 Ma for the basal Akchagylian transgression. Moreover, revision of the fossil content from the lowermost Akchagylian suggests the the intrabasinal origin of the transgression was likely triggered by a climatically-driven switch to a hydrologically-positive water budget in the Caspian region.

Revision of magnetostratigraphy in 18 sections from Turkmenistan that previously supported the “long Akchagylian” model (3.6–1.8 Ma) shows that the small reversed intervals correlated to Kaena and Mammoth subchrons and presented in six sections do not fulfil the criteria for such correlation. In particular, the reversed intervals are extremely short in relation to preceding and succeeding chrons, which cannot be explained by changes in lithology. We conclude that the base of the Akchagylian correlates to the upper Gauss chron and that reversed intervals likely represent geomagnetic excursions; one of them may correlate to the Porcupine excursion dated at 2.74 Ma.

Summarising the new and revised data, we propose new age constraints for the Akchagylian Stage of the Caspian Sea with following palaeoenvironmental episodes: 1. Akchagylian transgression at 2.95 ± 0.02 Ma occurring within the upper Gauss chron; 2. Akchagylian marine incursion characterising the establishment of the Caspian-Arctic hydrological connection at 2.75 Ma, also in the upper Gauss chron; 3. Termination of the Caspian-Arctic connection at ~2.45 Ma and transition to oligohaline environments; 4. First occurrence of indicative Apsheronian molluscs characterising the Akchagylian-Apsheronian boundary correlated to the Reunion (Feni) subchron at 2.13 Ma; 5. Rise of mesohaline biodiversity in the Caspian fossil record between 2.13 and 2.0 Ma suggesting the establishment of a Caspian-Black Sea hydrological connection.

The sudden expansion of the Capian Sea after a long-lasting lowstand at 2.95 ± 0.02 Ma likely reflects the rise of the atmospheric precipitation in the Eurasian interior linked to the interglacial intensification of the Atlantic Thermohaline Circulation between 2.95 and 2.82 Ma.

The Caspian and Caucasian regions being at the crossroads between Europe, Asia and Africa, comprise numerous important palaeontological and archaeological sites that define the biogeographic and anthropologic histories of Eurasia. The age constraints of many of these localities rely on the old Akchagylian age constraints that were proposed in the 70's of the last century. Our new integrated age constraints show that the ages of those localities should be carefully reviewed.

Declaration of Competing Interest

The authors declare that they have no known competing financial interests or personal relationships that could have appeared to influence the work reported in this paper.

Acknowledgements

We would like to thank Dr. Thomas Hoyle for scientific discussion on the topic of this manuscript. We are also thankful to Qucho and Maia Navrozashvili for amazing Georgian hospitality during our fieldwork. We are also very thankful to two anonymous reviewers whose critical reviews helped to improve the manuscript. At this historical time, we would also like to give our words of support to all people fighting against the COVID pandemic. This research is a part of the PRIDE project (Pontocaspian RIse and DEmise), which is funded by the European Union's Horizon 2020 Research and Innovation Program, under the Marie Skłodowska-Curie Action (grant agreement N° 642973).

Appendix A. Supplementary data

Supplementary data to this article can be found online at https://doi.org/10.1016/j.gloplacha.2021.103624.

References

Abdullayev, N.R., Riley, G.W., Bowman, A.P., 2012. Regional controls on lacustrine sandstone reservoirs: The Pliocene of the South Caspian Basin. In: Baganz, O.W., Bartov, Y., Bohacs, K.M., Nummedal, D. (Eds.), Lacustrine Sandstone Reservoirs and Hydrocarbon Systems. American Association of Petroleum Geologists.

Agustí, J., Vekua, A., Oms, O., Lordkipanidze, D., Bukhsianidze, M., Kiladze, G., Rook, L., 2009. The Pliocene-Pleistocene succession of Kvabebi (Georgia) and the background to the early human occupation of Southern Caucasus. Quat. Sci. Rev. 28, 3275–3280.

Alania, V.M., Chabukiani, A.O., Chagelishvili, R.L., Enukidze, O.V., Gogrichiani, K.O., Razmadze, A.N., Tsereteli, N.S., 2017. Growth structures, piggy-back basins and growth strata of the Georgian part of the Kura foreland fold–thrust belt: implications for late Alpine kinematic evolution. Geol. Soc. Lond., Spec. Publ. 428, 171–185.

Aliyeva, E.G.M., 2005. Reservoirs of the lower Pliocene Productive Series at the Western Flank of the South Caspian Basin. Lithol. Miner. Resour. 40, 267–278.

Ali-Zade, A.A., Alizade, K.A., Gabuniya, L.K., Negadaev-Nikonov, K.N., Nikiforova, K.V., 1972. International colloquium on the Neogene Quaternary boundary. Guidebook. Excursions in Moldavia, Georgia, Azerbaijan, May-June, 1972 (INQUA – IUGS Neogene Subcommission), Moscow.

Allen, M.B., Jones, S., Ismail-Zadeh, A., Simmons, M., Anderson, L., 2002. Onset of subduction as the cause of rapid Pliocene-Quaternary subsidence in the South Caspian basin. Geol 30, 775.

Allen, M.B., Vincent, S.J., Alsop, G., Ismail-Zadeh, A., Flecker, R., 2003. Late Cenozoic deformation in the South Caspian region: effects of a rigid basement block within a collision zone. Tectonophysics 366, 223–239.

Arslanov, N.V., Lokshin, A.V., Mamedov, A.V., 1988. On age constraints of Khazarian, Khvalynian and Neocaspian deposits of the Caspian Sea. Bull. Commiss. Study Quatern. Period 28–38.

Bartoli, G., Sarnthein, M., Weinelt, M., Erlenkeuser, H., Garbe-Schönberg, D., Lea, D.W., 2005. Final closure of Panama and the onset of northern hemisphere glaciation. Earth Planet. Sci. Lett. 237, 33–44.
Bista, D., 2019. Reconstructing the Pleistocene Connectivity History of the Black Sea and the Caspian Sea Using Strontium Iotopes. Doctoral thesis, Bristol.
Bukhsianidze, M., Koiava, K., 2018. Synopsis of the terrestrial vertebrate faunas from the Middle Kura Basin (Eastern Georgia and Western Azerbaijan, South Caucasus). Acta Palaeontol. Pol. 63.
Catuneanu, O., Abreu, V., Bhattacharya, J.P., Blum, M.D., Dalrymple, R.W., Eriksson, P. G., Fielding, C.R., Fisher, W.L., Galloway, W.E., Gibling, M.R., Giles, K.A., Holbrook, J.M., Jordan, R., Kendall, C., Macurda, B., Martinsen, O.J., Miall, A.D., Neal, J.E., Nummedal, D., Pomar, L., Posamentier, H.W., Pratt, B.R., Sarg, J.F., Shanley, K.W., Steel, R.J., Strasser, A., Tucker, M.E., Winker, C., 2009. Towards the standardization of sequence stratigraphy. Earth Sci. Rev. 92, 1–33.
Channell, J., Hodell, D.A., Curtis, J.H., 2016. Relative paleointensity (RPI) and oxygen isotope stratigraphy at IODP Site U1308: North Atlantic RPI stack for 1.2–2.2 Ma (NARPI-2200) and age of the Olduvai Subchron. Quat. Sci. Rev. 131, 1–19.
Cox, A., 1969. Geomagnetic reversals. Science (New York, N.Y.) 163, 237–245.
Danukalova, G.A., 1996. Bivalves and Stratigraphy of the Akchagylian. Nauka, Moscow, 104, XXIV Seiten, Seite 105-130.
de Schepper, S., Gibbard, P.L., Salzmann, U., Ehlers, J., 2014. A global synthesis of the marine and terrestrial evidence for glaciation during the Pliocene Epoch. Earth Sci. Rev. 135, 83–102.
Derevianko, A., Anoykin, A., Kazansky, A., Matasova, G., 2015. New Data to Justify the Age of Early Paleolithic Artifacts of Rubas-1 Site (Seaside Dagestan). Izvasu. https://doi.org/10.14258/izvasu(2015)3.2-11.
Djikia, N., 1968. Historical Development of Akchagylian Malacofauna from Eastern Georgia.: (in Russian). Mecniereba, Tbilisi.
Driscoll, N.W., Haug, G.H., 1998. A short circuit in thermohaline circulation: a cause for northern hemisphere glaciation? Science (New York, N.Y.) 282, 436–438.
Fisher, R., 1953. Dispersion on a sphere. Proc. Royal Soc. A: Math. Phys. Eng. Sci. 217, 295–305.
Forte, A.M., Sumner, D.Y., Cowgill, E., Stoica, M., Murtuzayev, I., Kangarli, T., Elashvili, M., Godoladze, T., Javakhishvili, Z., 2015. Late Miocene to Pliocene stratigraphy of the Kura Basin, a subbasin of the South Caspian Basin: Implications for the diachroneity of stage boundaries. Basin Res. 27, 247–271.
Gibbard, P.L., Head, M.J., 2020. The quaternary period. In: Geologic Time Scale 2020, pp. 1217–1255.
Gladenkov, A.Y. (Ed.), 2018. Neogene and Quaternary of Russia: Stratigraphy, Events and Paleogeography. GEOS, Moscow.
Gurarii, G.Z., 2015. Some data on the characteristics of the geomagnetic field at the Gauss–Matuyama magnetic chron boundary from the Pirnuar section, West Turkmenistan. Izv. Phys. Solid Earth 51, 651–673.
Haug, G.H., Tiedemann, R., 1998. Effect of the formation of the Isthmus of Panama on Atlantic Ocean thermohaline circulation. Nature 393, 673–676.
Haywood, A.M., Dowsett, H.J., Dolan, A.M., 2016. Integrating geological archives and climate models for the mid-Pliocene warm period. Nat. Commun. 7, 10646.
Hoyle, T.M., 2019. Biotic Change and Landlocked Seas: Ecosystem Responses to Climate and Sea Level Variability in the Plio-Pleistocene of the Pontocaspian Basins. Utrecht University, Faculty of Geosciences, Department of Earth Sciences, Utrecht, p. 244.
Hoyle, T.M., Leroy, S.A., López-Merino, L., Miggins, D.P., Koppers, A.A., 2020. Vegetation succession and climate change across the Plio-Pleistocene transition in eastern Azerbaijan, Central Eurasia (2.77–2.45 Ma). Palaeogeogr. Palaeoclimatol. Palaeoecol. 538, 109386.
Hoyle, T.M., Leroy, S.A.G., Lopez-Merino, L., van Baak, C., Cortizas, A.M., Richards, K., Aghayeva, V., 2021. Biological turnovers in response to marine incursion into the Caspian Sea at the Plio-Pleistocene transition. Glob. Planet. Chang. https://doi.org/10.1016/j.gloplacha.2021.103623.
Jackson, J., Priestley, K., Allen, M., Berberian, M., 2002. Active tectonics of the South Caspian Basin. Geophys. J. Int. 148, 214–245.
Jorissen, E., Abels, H., Wesselingh, F., Lazarev, S., Aghayeva, V., Krijgsman, W., 2019. Amplitude, frequency and drivers of Caspian Sea lake-level variations during the early Pleistocene and their impact on a protected wave-dominated coastline. Sedimentology. https://doi.org/10.1111/sed.12658.
Jorissen, E.L., 2020. The Pontocaspian Basins in a Grain of Sand: Coastal Sedimentary Architecture, Forcing Mechanisms, and Faunal Turnover Events in Restricted Basins. PhD, Utrecht.
Khain, V.E., Bogdanov, V.I., Popkov, V.I., Chekhovich, P.A., 2004. Major geostructures and basic features of the development of Caspian oil and gas megabasins. Ecol. Bull. Res. Cent. Black Sea Econ. Cooperat. 47–56.
Khramov, A.N., 1960. Paleomagnetism and Stratigraphic Correlation (Canberra).
Khramov, A.N., 1963. Paleomagnetic sections of Pliocene and Post-Pliocene of the Apsheronsk-Trancaucasian region and their correlation. In: Proceedings of the all Union Petroleum Research Exploration Institute (VNIGRI), pp. 253–262.
King, R.F., 1955. The remanent magnetism of artificially deposited sediments. Geophys. J. Int. 7, 115–134.
Koppers, A.A., 2002. ArArCALC—software for 40Ar/39Ar age calculations. Comput. Geosci. 28, 605–619.
Koymans, M.R., Langereis, C.G., Pastor-Galan, D., Hinsbergen, D., 2016. Paleomagnetism.org: an online multi-platform open source environment for paleomagnetic data analysis. Comput. Geosci. 93, 127–137.
Krijgsman, W., Stoica, M., Vasiliev, I., Popov, V.V., 2010. Rise and fall of the Paratethys Sea during the Messinian Salinity Crisis. Earth Planet. Sci. Lett. 290, 183–191.
Krijgsman, W., Tesakov, A., Yanina, T., Lazarev, S., Danukalova, G., van Baak, C., Agustí, J., Alçiçek, M.C., Aliyeva, E., Bista, D., Bruch, A., Büyükmeriç, Y., Bukhsianidze, M., Flecker, R., Frolov, P., Hoyle, T.M., Jorissen, E.L., Kirscher, U., Koriche, S.A., Kroonenberg, S.B., Lordkipanidze, D., Oms, O., Rausch, L., Singarayer, J., Stoica, M., van de Velde, S., Titov, V.V., Wesselingh, F.P., 2019. Quaternary time scales for the Pontocaspian domain: Interbasinal connectivity and faunal evolution. Earth Sci. Rev. 188, 1–40.
Krijgsman, W., Palcu, D.V., Andreetto, F., Stoica, M., Mandic, O., 2020. Changing seas in the late Miocene Northern Aegean: a Paratethyan approach to Mediterranean basin evolution. Earth Sci. Rev. 210, 103386.
Kroonenberg, S.B., Alekseevski, N.I., Aliyeva, E.G.M., Allen, M.B., Aybulatov, D.N., Baba-Zadeh, A., Badyukova, E.N., Davies, C.E., Hinds, D.J., Hoogendoorn, R.M., Huseynov, D., Ibrahimov, B., Mamedov, P., Overeem, I., Rusakov, G.V., Suleymanov, S., Svitoch, A.A., Vincent, S.J., 2005. Two deltas, two basins, one river, one sea: the modern Volga delta as an analogue of the Neogene Productive Series, South Caspian Basin. In: Giosan, L., Bhattacharya, J.P. (Eds.), River Deltas-Concepts, Models and Examples, pp. 231–255.
Kuiper, K.F., Deino, A., Hilgen, F.J., Krijgsman, W., Renne, P.R., Wijbrans, J.R., 2008. Synchronizing rock clocks of Earth history. Science (New York, N.Y.) 320, 500–504.
Langereis, C.G., Krijgsman, W., Muttoni, G., Menning, M., 2010. Magnetostratigraphy – concepts, definitions, and applications. Newsl. Stratigr. 43, 207–233.
Lawrence, K.T., Herbert, T.D., Brown, C.M., Raymo, M.E., Haywood, A.M., 2009. High-amplitude variations in North Atlantic Sea surface temperature during the early Pliocene warm period. Paleoceanography 24.
Lazarev, S., Jorissen, E.L., van de Velde, S., Rausch, L., Stoica, M., Wesselingh, F.P., van Baak, C.G., Yanina, T.A., Aliyeva, E., Krijgsman, W., 2019. Magneto-biostratigraphic age constraints on the palaeoenvironmental evolution of the South Caspian basin during the Early-Middle Pleistocene (Kura basin, Azerbaijan). Quat. Sci. Rev. 222, 105895.
Lebedeva, N.A., 1972. About geological position of terestrial mammal faunas of Khaprovian, Tamanian and Tiraspoian faunal complexes in Akchagylian and Apsheronian marine layers of the East Transcaucasia. Bull. Comiss. Study Quatern. 99–115.
Lee, J.-Y., Marti, K., Severinghaus, J.P., Kawamura, K., Yoo, H.-S., Lee, J.B., Kim, J.S., 2006. A redetermination of the isotopic abundances of atmospheric Ar. Geochim. Cosmochim. Acta 70, 4507–4512.
Lisiecki, L.E., Raymo, M.E., 2005. A Pliocene-Pleistocene stack of 57 globally distributed benthic δ18O records. Paleoceanography 20.
Mangino, S., Priestley, K., 1998. The crustal structure of the southern Caspian region. Geophys. J. Int. 133, 630–648.
McFadden, P.L., McElhinny, M.W., 1990. Classification of the reversal test in palaeomagnetism. Geophys. J. Int. 103, 725–729.
Min, K., Mundil, R., Renne, P.R., Ludwig, K.R., 2000. A test for systematic errors in 40Ar/39Ar geochronology through comparison with U/Pb analysis of a 1.1-Ga rhyolite. Geochim. Cosmochim. Acta 64, 73–98.
Morton, A., Allen, M., Simmons, M., Spathopoulos, F., Still, J., Hinds, D., Ismail-Zadeh, A., Kroonenberg, S., 2003. Provenance patterns in a neotectonic basin: Pliocene and Quaternary sediment supply to the South Caspian. Basin Res. 15, 321–337.
Naidina, O.D., Richards, K., 2016. Pollen evidence for late Pliocene – early Pleistocene vegetation and climate change in the North Caucasus, North-Western Caspian Region. Quat. Int. 409, 50–60.
Nevesskaya, L.A., Goncharova, I.A., Ilyina, L.B., Paramonova, N.P., Khondkarian, S.O., 2003. The neogene stratigraphic scale of the eastern paratethys. Stratigr. Geol. Correl. 11, 105–127.
Nevesskaya, L.A., Kovalenko, E.I., Beluzhenko, E.V., Popov, S.V., Goncharova, I.A., Danukalova, G.A., Zhidovinov, I.Y., Zaytsev, A.V., Zastrozhnov, A.S., Ilyina, L.B., Paramonova, N.P., Pinchuk, T.N., Pismennaya, N.S., Agadjanian, A.K., Lopatin, A.V., Trubikhin, V.M., 2004. Explanatory Letter to the Regional Unified Stratigraphic Scheme of Neogene Deposits of the Southern Regions of the European Part of Russia, Moscow.
Palo, J.U., Väinölä, R., 2006. The enigma of the landlocked Baikal and Caspian seals addressed through phylogeny of phocine mitochondrial sequences. Biol. J. Linn. Soc. 88, 61–72.
Paramonova, N.P., 1994. History of Sarmatian and Akchagylian Bivalves. Nauka, Moscow.
Pevzner, M.A., 1986. Stratigraphy of the Middle Miocene - Pliocene of the South Europe (Based on Paleomagnetic Data). Dissertation, Moscow.
Phillips, D., Matchan, E.L., 2013. Ultra-high precision 40Ar/39Ar ages for fish Canyon Tuff and Alder Creek Rhyolite sanidine: New dating standards required? Geochim. Cosmochim. Acta 121, 229–239.
Popov, S.V., Shcherba, I.G., Ilyina, L.B., Nevesskaya, L.A., Paramonova, N.P., Khondkarian, S.O., Magyar, I., 2006. Late Miocene to Pliocene palaeogeography of the Paratethys and its relation to the Mediterranean. Palaeogeogr. Palaeoclimatol. Palaeoecol. 238, 91–106.
Popov, S.V., Antipov, M.P., Zastrozhnov, A.S., Kurina, E.E., Pinchuk, T.N., 2010. Sea-level fluctuations on the northern shelf of the Eastern Paratethys in the Oligocene-Neogene. Stratigr. Geol. Correl. 18, 200–224.
Raffi, I., Wade, B.S., Pälike, H., Beu, A.G., Cooper, R., Crundwell, M.P., Krijgsman, W., Moore, T., Raine, I., Sardella, R., Vernyhorova, Y.V., 2020. The neogene period. In: Geologic Time Scale 2020, pp. 1141–1215.
Reynolds, A.D., Simmons, M.D., Bowman, M.B.J., Henton, J., Brayshaw, A.C., Ali-Zade, A.A., Guliyev, I.S., Suleymanova, S.F., Ateava, E.Z., Mamedova, D.N., Koshkarly, R.O., 1998. Implications of outcrop geology for reservoirs in the neogene productive series: apsheron Peninsula, Azerbaijan. AAPG Bull. 82, 25–49.
Richards, K., van Baak, C.G., Athersuch, J., Hoyle, T.M., Stoica, M., Austin, W.E., Cage, A.G., Wonders, A.A., Marret, F., Pinnington, C.A., 2018. Palynology and micropalaeontology of the Pliocene - Pleistocene transition in outcrop from the

western Caspian Sea, Azerbaijan: potential links with the Mediterranean, Black Sea and the Arctic Ocean? Palaeogeogr. Palaeoclimatol. Palaeoecol. 511, 119–143.
Richards, K., Vincent, S.J., Davies, C.E., Hinds, D.J., Aliyeva, E., 2021. Palynology and sedimentology of the Pliocene Productive Series from eastern Azerbaijan. Palynology 1–36.
Shantser, E.V. (Ed.), 1982. Stratigraphy of the USSR: Quaternary System. Nedra, Moscow.
Svitoch, A.A., 2014. The Great Caspian Sea: Structure and History. Moscow State University, Moscow, p. 270.
Svitoch, A.A., Yanina, T.A., Novikova, N.G., Sobolev, V.M., Khomenko, A.A., 2010. The Pleistocene of the Manych: (Structure and Evolution). Geographical faculty MSU, Moscow.
Taner, G., 1997. Das Pliozän des östlichen Dardanellen-Beckens. Molluskenfauna und Stratigraphie. Annalen des Naturhistorischen Museum in Wien, Türkei, pp. 35–67.
Tauxe, L., 2010. Essentials of Paleomagnetism. University of California Press, Berkeley.
Tauxe, L., Kent, D.V., 2004. A Simplified Statistical Model for the Geomagnetic Field and the Detection of Shallow Bias in Paleomagnetic Inclinations: Was the Ancient magnetic Field Dipolar? In: Channell, J., Kent, D.V., Lowrie, W., Meert, J.G. (Eds.), Timescales of the Paleomagnetic Field. American Geophysical Union, Washington, D. C, pp. 101–115.
Tesakov, A.S., 2004. Biostratigrafija srednego pliocena-ėoplejstocena Vostočnoj Evropy: (po melkim mlekopitajuščim). Nauka, Moskva, p. 246.
Torres, M.A., 2007. The Petroleum Geology of Western Turkmenistan: The Gograndag-Okarem Province. In: Isaksen, G.H. (Ed.), Yilmaz, P.O. Oil and Gas of the Greater Caspian Area, American Association of Petroleum Geologists, pp. 1–24.
Trubikhin, V.M., 1977. Paleomagnetism and Stratigraphy of Akchagylian Deposits of West Turkmenia (Moscow).
Väinölä, R., 1995. Origin and recent Endemic Divergence of a Caspian Mysis Species Flock with Affinities to the "Glacial Relict" Crustaceans in Boreal Lakes. Evolution 49, 1215.
van Baak, C., 2015. Mediterranean-Paratethys Connectivity during the Late Miocene to Recent: Unravelling Geodynamic and Paleoclimatic Causes of Sea-Level Change in Semi-Isolated Basins. Doctoral dissertation, Utrecht.
van Baak, C., Vasiliev, I., Stoica, M., Kuiper, K.F., Forte, A.M., Aliyeva, E., Krijgsman, W., 2013. A magnetostratigraphic time frame for Plio-Pleistocene transgressions in the South Caspian Basin, Azerbaijan. Glob. Planet. Chang. 103, 119–134.
van Baak, C., Grothe, A., Richards, K., Stoica, M., Aliyeva, E., Davies, G., Kuiper, K.F., Krijgsman, W., 2019. Flooding of the Caspian Sea at the intensification of Northern Hemisphere Glaciations. Glob. Planet. Chang. 174, 153–163.
van Baak, C.G., Stoica, M., Grothe, A., Aliyeva, E., Krijgsman, W., 2016. Mediterranean-Paratethys connectivity during the Messinian salinity crisis: the Pontian of Azerbaijan. Glob. Planet. Chang. 141, 63–81.
Vandendorpe, J., van Baak, C.G.C., Stelbrink, B., Delicado, D., Albrecht, C., Wilke, T., 2019. Historical faunal exchange between the Pontocaspian Basin and North America. Ecol. Evolut. 9, 10816–10827.
Vardanyan, A.A., Minasyan, D.O., Nechaeva, T.B., 2003. On a possibility to identify paleo-secular variations of geomagnetic field in the Matuyama epoch. Proceedings of the NAS RA: Earth Sciences 56.
Vekua, A., 1972. Kvabebi Fauna of Akchagylian Vertebrates: (in Russian). Nauka, Moscow.
Vereshchagin, V.N. (Ed.), 1982. Stratigraphic Dictionary of the USSR: Paleogene, Neogene, Quaternary System. Nedra, Leningrad.
Vincent, S.J., Davies, C.E., Richards, K., Aliyeva, E., 2010. Contrasting Pliocene fluvial depositional systems within the rapidly subsiding South Caspian Basin; a case study of the palaeo-Volga and palaeo-Kura river systems in the Surakhany Suite, Upper Productive Series, onshore Azerbaijan. Mar. Pet. Geol. 27, 2079–2106.
Vinogradov, A.P., 1969. Atlas of Lithological-Paleogeographical Maps of the Soviet Union. Moscow, Vses. Aerogeol. Trest Mingeol. SSSR.
Yakhimovich, V.L., Suleymanova, F.I., 1981. Magnetostratigraphic section of the Pliocene and lower Pleistocene of the non-glacial zone of the Pre-Urals. Bull. Commiss. Study Quatern. Period 31–37.
Zastrozhnov, A., Danukalova, G., Golovachev, M., Osipova, E., Kurmanov, R., Zenina, M., Zastrozhnov, D., Kovalchuk, O., Yakovlev, A., Titov, V., Yakovleva, T., Gimranov, D., 2021. Pleistocene palaeoenvironments in the lower Volga region (Russia): Insights from a comprehensive biostratigraphical study of the seroglazovka locality. Quat. Int. https://doi.org/10.1016/j.quaint.2020.12.039.
Zastrozhnov, A.S., Shkatova, V.K., Minina, E.A., Tarnogradskiy, V.D., Astakhov, V.I., Gusev, E.A., 2013. Map of Quaternary deposits of the Russian Federation. Scale 1: 250000: Explanatory letter. Ministry of nature of Russia, Rosnedra, VSEGEI, All Russian Research Institute of Geology and Mineral Resources of the Ocean, Saint Petersburg.
Zubakov, V.A., 2001. History and causes of variations in the Caspian Sea level: the Mio-Pliocene, 7.1–1.95 Million years ago. Water Res. 28, 249–256.
Zubakov, V.A., Borzenkova, I.I., 1990. Global Palaeoclimate of the Late Cenozoic. Elsevier, Amsterdam, p. 456.
Zubakov, V.A., Kochegura, V.V., 1976. Magnetochronological scale of the latest stage (5 Ma). Geomagnet. Res. 37–44.